Université Mohamed Khider de Biskra
Faculté des Sciences et de la Technologie
Département de Génie Mécanique

MÉMOIRE DE MASTER

Domaine : Sciences et Techniques
Filière : Génie Mécanique
Spécialité : Energétique

Réf. : ......

Présenté et soutenu par :
Mr. Rezeq Abuhasnah

Le : 10 Juillet 2019

Experimental study of the thermal performance and effectiveness efficiency of a flat plate solar collector.

Jury :

Dr.	Lakhdar Sedira	MCA	Université de Biskra	Président
Pr.	Abdelhafid Moummi	Pr	Université de Biskra	Examinateur
Dr.	Adnane Labed	MCA	Université de Biskra	Rapporteur

Année universitaire : 2018 - 2019

Dedication

I dedicate this work to my dear mother

My dear father

My brothers Ashraf and Aws

My sisters

My friends each with his name

To my supervisor

To all my teachers each in his name

Acknowledgement

I thank God, above all, to allow me to achieve this work with patience and perseverance.

I would like to thank my parents for their love and support, especially within my last three months of graduate studies. I thank also, my supervisor Dr. Adnane Labed for his time, help and efforts.

Finally, I thank all my teachers, colleagues and all the administrative and technical staff of the department of mechanical engineering of the University of Biskra, Algeria.

List of Figures

Chapter I

Chapter II

Chapter III

List of Tables

Chapter II

Nomenclature

m Air mass flow rate (kg /s).

G Global irradiance incident on solar air heater collector (W/m²).

Q_U Useful energy gain of the collector (W/m²).

T_{in} Inlet air temperature of the collector (◦C).

T_{out} Outlet fluid temperature of the collector (◦C).

C_{p-air} Specific heat of air at constant pressure (J/kg.k).

ɳ   Thermal efficiency (%).

A Collector surface area (m²).

S   Tube area of the vacuum cleaner (m²).

ρ   Density (kg/m³).

v Velocity (m/s).

TR $\Delta T/G$ (m².◦C/w).

E   Electrical consumption (w).

K   Thermal conductivity (W/m.k).

D   Diameter (m).

L   Length (m).

W   width (m).

Greek letters

α   Absorption.

ε   Emissivity.

τ   Transmission.

β   Angle of inclination (degree/rad).

ϕ   Latitude of the site (degree).

Summary

Chapter I : Bibliographic study

Chapter II : Experimental setup

Chapter III : Results and discussion

Introduction

Introduction

The world energy consumption in the last half-century has rapidly increased and is expected to continue to grow over the next 50 years but with significant differences. Additional factors make the picture more complex. These additional complicating factors represent approximately one-third of the world's population. On the positive side, the renewable energy (RE) technologies, solar thermal and photovoltaic (PV) are finally showing maturity and the ultimate promise of cost competitiveness [1].

The transformation of solar radiation into thermal energy is based on systems known as solar collectors. This energy is used directly by relying on so-called passive systems by storing it in building elements (veranda, greenhouse, facade glazed) or indirectly through so-called active solar collector systems by means of a coolant that can be water or air. They are used for heating buildings and for drying food and food products. These systems are composed of a black plate called absorber. The absorber is covered with a glazing that is transparent to incoming radiation and opaque to the infra-red radiation emitted by the black plate. A heat transfer fluid circulates either under the absorber. These solar collectors can take various forms and arrangements depending on the design geometry [2].

The main objective of this thesis is to investigate the thermal performance and the effectiveness efficiency of simple solar air heater (without fins) with different air flow rate .

This thesis is articulated in three chapters:

The first chapter presents the solar collector in a general way, its components, its different types. Then, we expose a bibliographical analysis of some works related with our study.

In the second chapter we describe in detail of the experimental setup, the measuring instruments used, and the test procedure.

 The third chapter presents the results of tests and measurements: solar radiation, temperatures, speeds of wind as well as the thermal performances analysis, comparison and interpretation.

Finally a general conclusion that encompasses the most important information included in this thesis is written at the end of this manuscript.

Chapter I:

Bibliographic study

I.1. Introduction

Over long run the continued consumption of fossil fuels at ever increasing rates presents clear environment hazards and escalating economic and social costs, which make the development of alternate sources of energy almost essential. So the world is turning to solar energy [3].

Solar thermal energy has been used for centuries by ancient people's harnessing solar energy for heating and drying. More recently, in a wide variety of thermal processes solar energy has been developed for power generation, water heating, mechanical crop drying, and water purification, among others [4].

In this chapter we are interesting in the works investigating the thermal performances of solar air flat plate collectors, the presentation of some types of solar collectors and the explication of its working principle.

I.2. Different types of solar collectors

Solar collectors are recognized as low-, medium-, or high-temperature heat exchangers. There are several types of thermal solar collectors:

- Flat-plate solar collectors.
- Concentrating collectors (parabolic / cylinder parabolic).
- Evacuated-tube collectors.
- Transpired air collectors.

The basic principle of solar thermal collection is that when solar radiation strikes a surface, a part of it is absorbed, thereby increasing the temperature of the surface. The efficiency of that surface as a solar collector depends not only on the absorption efficiency but also on how the thermal and eradiation losses to the surroundings are minimized and how the energy from the collector is removed for useful purposes [1].

- Flat-plate solar collectors:

Figure I.1 : Flat plate solar collector.

- Evacuated-tube collectors:

This type of solar collector uses a series of evacuated tubes to heat water for use. These tubes utilize a vacuum, or evacuated space, to capture the suns energy while minimizing the loss of heat to the surroundings. They have an inner metal tube which acts as the absorber plate, which is connected to a heat pipe to carry the heat collected from the Sun to the water. This heat pipe is essentially a pipe where the fluid contents are under a very particular pressure. At this pressure, the "hot" end of the pipe has boiling liquid in it while the "cold" end has condensing vapor. This allows for thermal energy to move more efficiently from one end of the pipe to the other. Once the heat from the Sun moves from the hot end of the heat pipe to the condensing end, the thermal energy is transported into the water being heated for use [5].

Figure I.2: Evacuated-tube collectors.

- Concentrating collectors:

In order to deliver high temperatures with good efficiency a high performance solar collector is required. Systems with light structures and low cost technology for process heat applications up to 400 ◦C could be obtained with parabolic through collectors (PTCs). PTCs can effectively produce heat at temperatures between 50 and 400 ◦C [6].
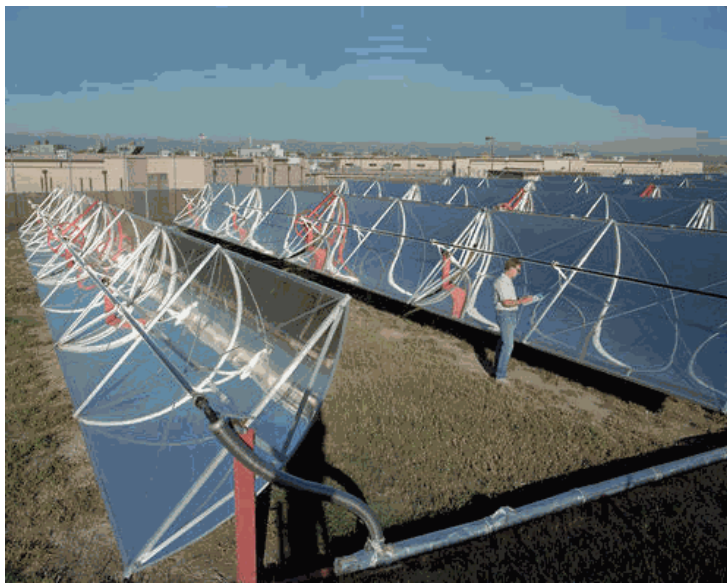
Figure I.3: Concentrating collectors(cylinder parabolic).

- Transpired air collectors:

Transpired air collectors use a simple, elegant technology to capture the sun's heat to warm buildings. The collectors consist of dark, perforated metal plates installed over a building's south-facing wall. An air space is created between the old wall and the new facade. The dark outer facade absorbs solar energy and rapidly heats up on sunny days – even when the outside air is cold.

A fan or blower draws ventilation air into the building through hundreds of tiny holes in the collectors and up through the air space between the collectors and the south wall. The solar energy absorbed by the collectors warms the air flowing through them by as much as 40°F [7].
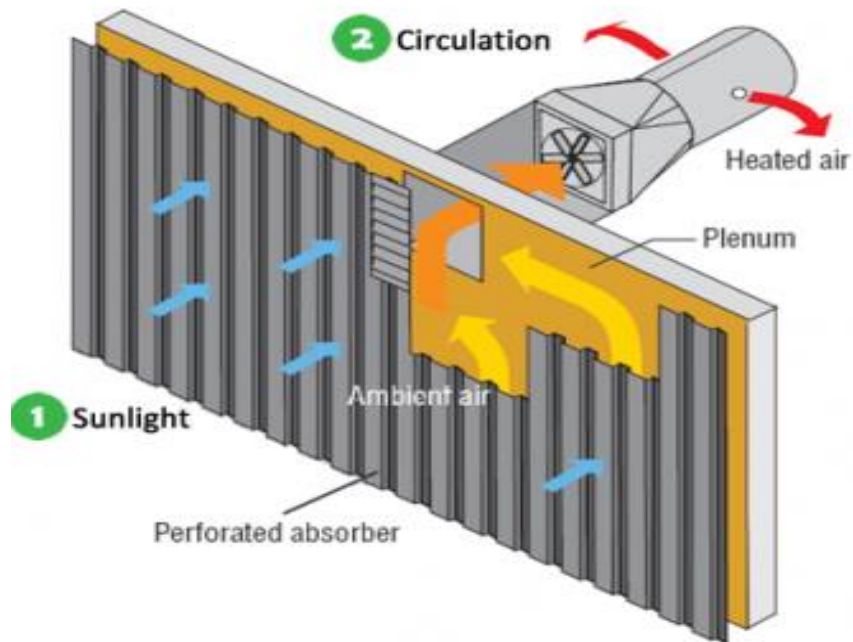
Figure I.4: Transpired air collectors.

I.3. Flat-Plate Collectors

The flat plate solar collector is most common solar thermal device and has been used for many decades. A flat plate collector consists of an absorber, a transparent cover, a frame and, commonly, insulation. Usually a low-iron tempered glass is used as a transparent cover. The absorber surface is the heart of the flat plate solar collector and is typically made of copper or

aluminum and painted black or selectively coated. When used, insulation is located at the back and sides of the collector to limit heat losses. The most common insulations material for flat plate collectors are polyurethane and mineral wool. A frame of tubes is attached to the absorber surface to allow for the flow of a heat transfer fluid. The thermal efficiency of this collector type normally ranges from 40% to 60% for the low- to medium-temperature applications, and decreases rapidly as temperatures exceed 60∘C. These collectors are generally used for temperatures less than 100∘C and a preferred choice for combined photovoltaic thermal modules [8].These collectors are of two basic types based on the heat-transfer fluid [1]:

1. Liquid type: where heat-transfer fluid may be water, mixture of water and antifreeze oil is shown in figure 5.
2. Air type: where heat-transfer medium is air (used mainly for drying and space heating requirements) this type shown in figure 6.
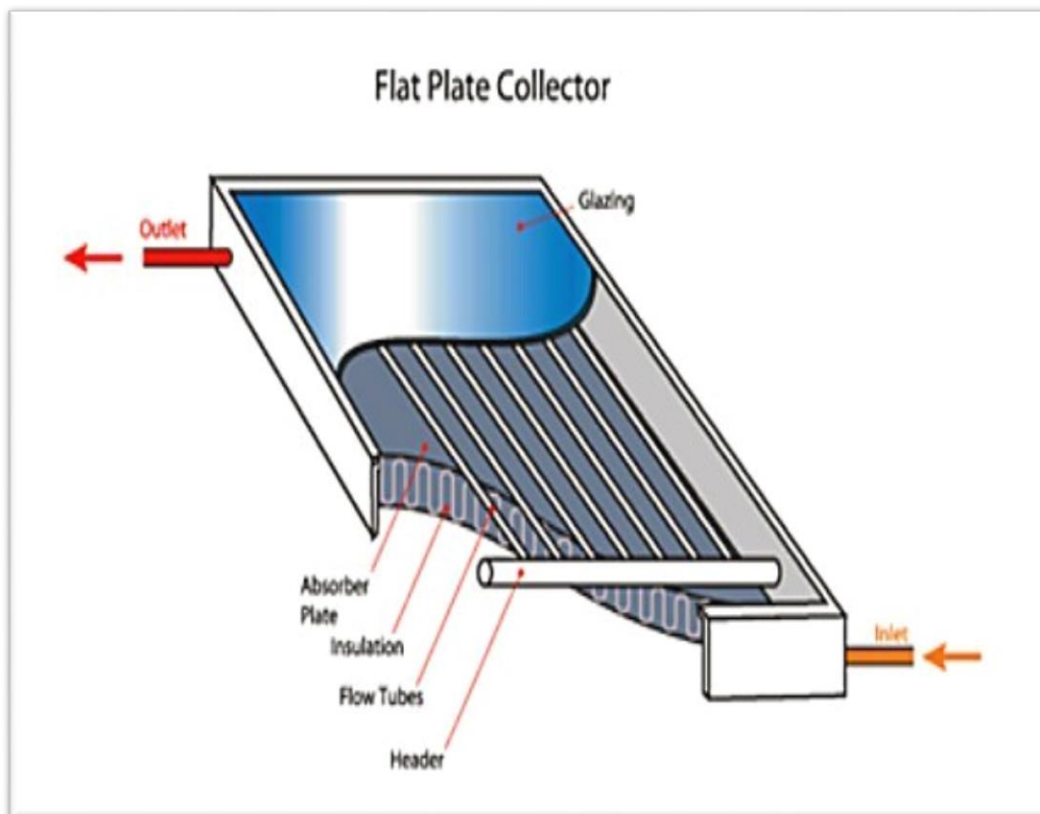
Figure I.5: Flat-Plate Collector (liquid type).
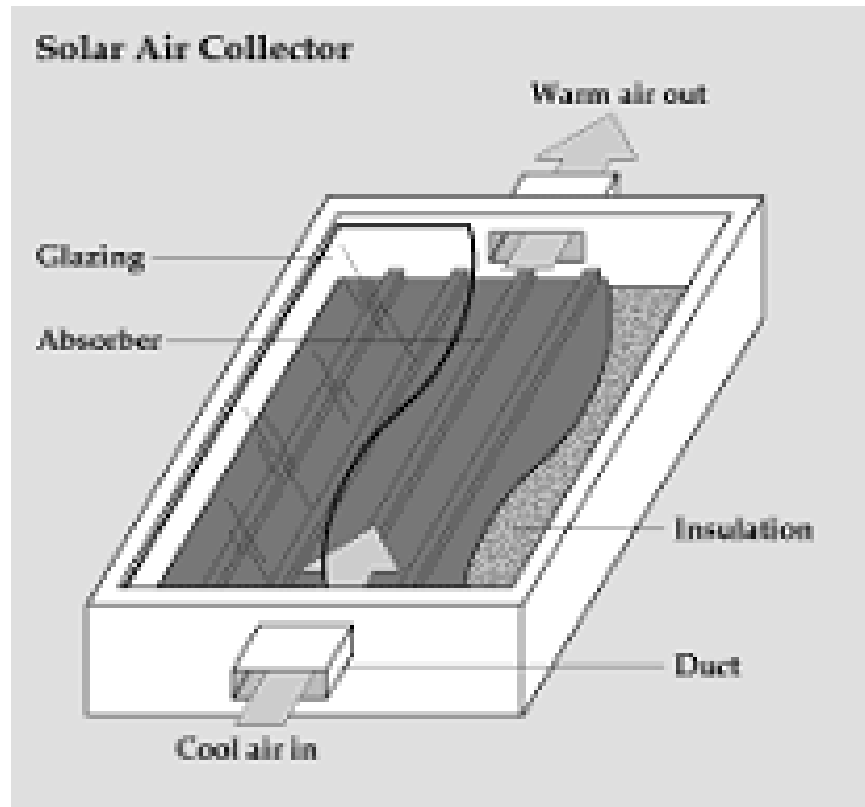
Figure I.6: Flat-Plate Collector (air type).

I.4. Previous studies about Flat-Plate Collectors

This part investigates some previous studies from the literature about solar Flat-Plate Collectors**:**

The study **of A. Fudholi and K. Sopian** [9]**,** presents the fundamental mechanisms and descriptions of solar collectors, which are indispensable components of solar dryers. Then, analysis techniques generally used for the evaluation of solar collector performance, especially energy analysis and exergy analysis, are reported. Experimental and theoretical results from their studies on the performance levels of solar air flat plate collectors are summarized as well. During indoor testing, the energy and exergy efficiencies of solar air flat plate collectors range from 30% to 79% and from 8% to 61%, respectively. Different solar collectors are depicted and classified and the designs and performance levels of solar collectors with fins integrated to a fluidized bed combination of heat pump and biomass furnace are also reported. Moreover, solar air flat plate

collector performances in the drying application of marine and agricultural products a presented. The energy and exergy efficiency of the solar air flat plate collector in the drying application (outdoor testing) range from 28% to 62% and from 30% to 57%, respectively.

Chabane et al [10], investigated experimentally the thermal performance of a single pass solar air heater with fins attached, they compared between the solar collectors with fins and without fins to find that fins enhanced the thermal efficiency. Experiments were performed for an air mass flow rate of 0.012 kg/s. The maximum efficiency levels obtained for the 0.012 kg/s with and without fins were 40.02% and 34.92% respectively. They noted that the highest collector efficiency and air temperature rise were achieved by the finned collector with an angle of 45, whereas the lowest values were obtained from the collector without fins. The efficiency of the solar air collectors depends significantly on the solar radiation and surface geometry of the collectors and the fins on the back of the absorber plate.
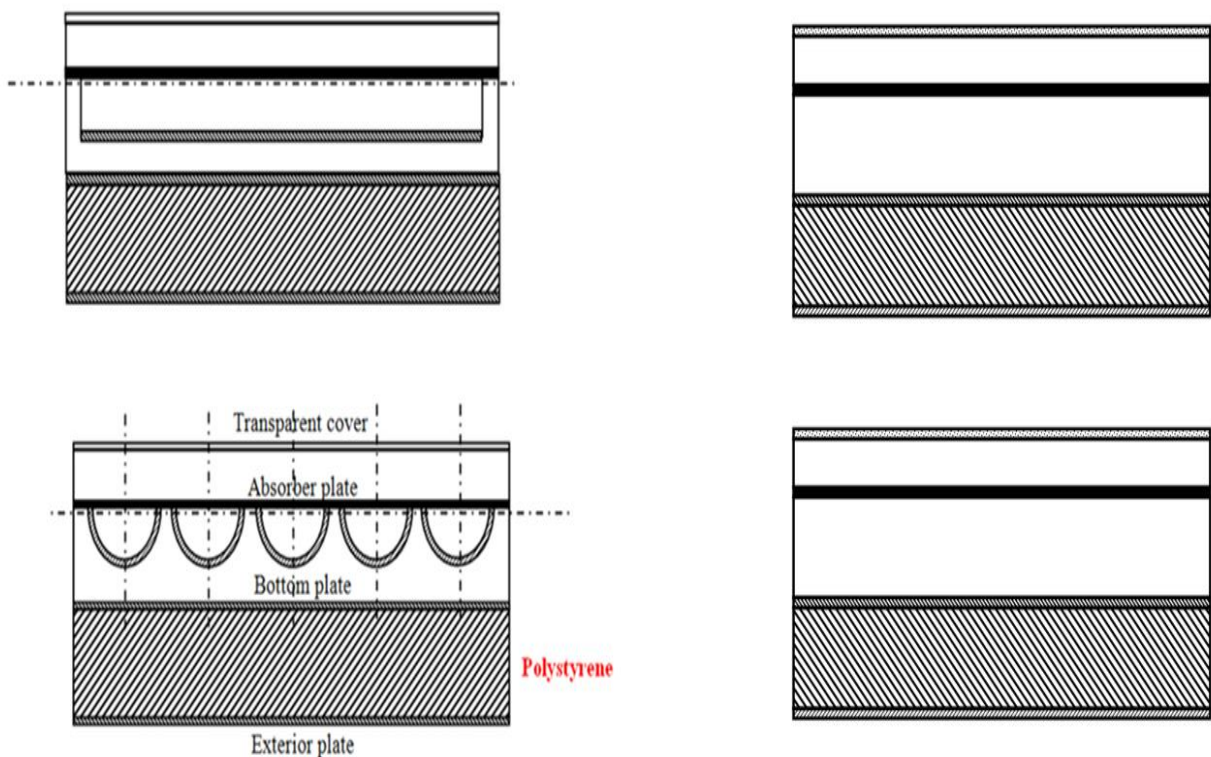
Figure I.7: Composition of solar box with and without fins [10].
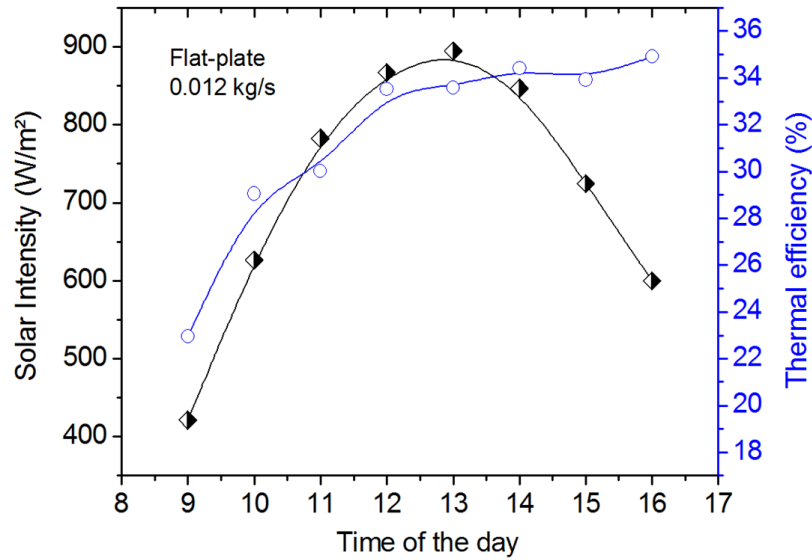
Figure I.8: Solar intensity and thermal efficiency versus time of day for a single pass solar air heater, with flow rates at 0.012 kg/s, corresponding to solar collectors without fins [10].
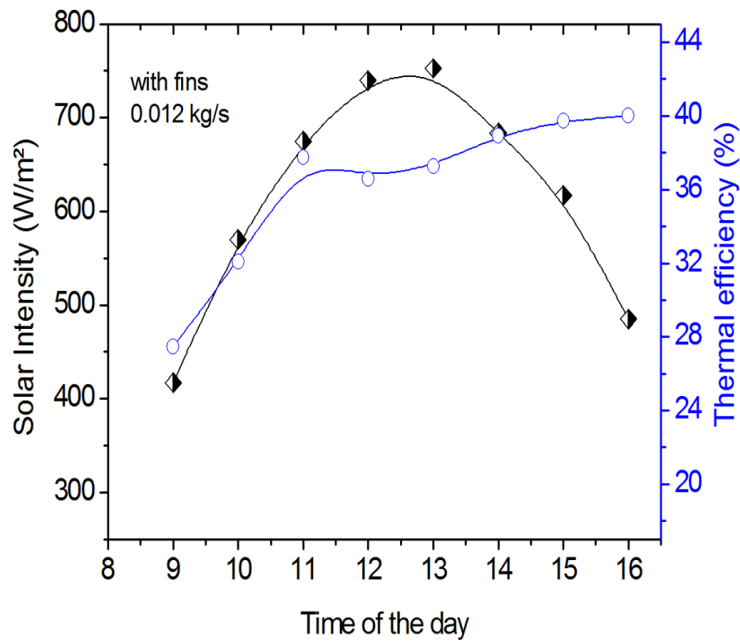
Figure I.9: Solar intensity and thermal efficiency versus time of day for a single pass solar air heater, with flow rates at 0.012 kg/s, corresponding to solar collectors with fins [10].

Labed et al [11], presented an experimental investigation the performances of FPC and its application in drying: first, the best performing solar dryer is selected between two models of flat plate solar collectors (FPCs). The second part investigates the drying behavior of henna (Lawsonia alba, syn. Lawsonia inermis Linn.) using the best selected FPC. They used two models of flat plate solar collectors, the first one is a simple-pass collector with trapezoidal obstacles (modelI),the second one is a double pass collector with trapezoidal obstacles in the air flow duct (model II) the two models is shown in figure 10. The first examination has enabled us to demonstrate that, at different air mass flow, the highest efficiencies are obtained from the double pass solar air FPC with trapezoidal obstacles. In addition, the use of the best performing FPC (model II) reduces 20% of henna drying time in comparison with model I and 75% comparing to the traditional drying. The effect of the air mass flow rate is also studied to find the optimum drying air rate. It is clear that drying time with 0.024 kg/s is shorter than those with 0.012 and 0.036 kg/s. the increase in the initial product quantity increases the total drying time. It could be concluded that, the use of solar dryers allows us to avoid the mixture of henna leaves with the ground during drying and also prevents the penetration of insects and scorpions in the dried samples.
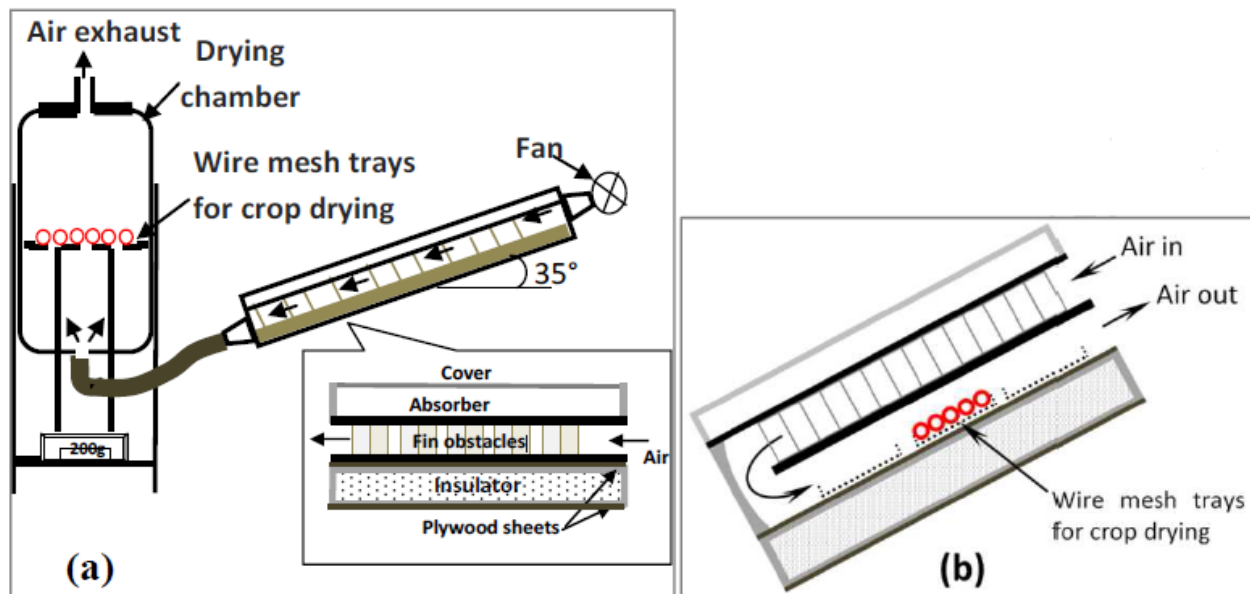
Figure I.10: Experimental devices for henna drying; a) model I, b) model II [11].
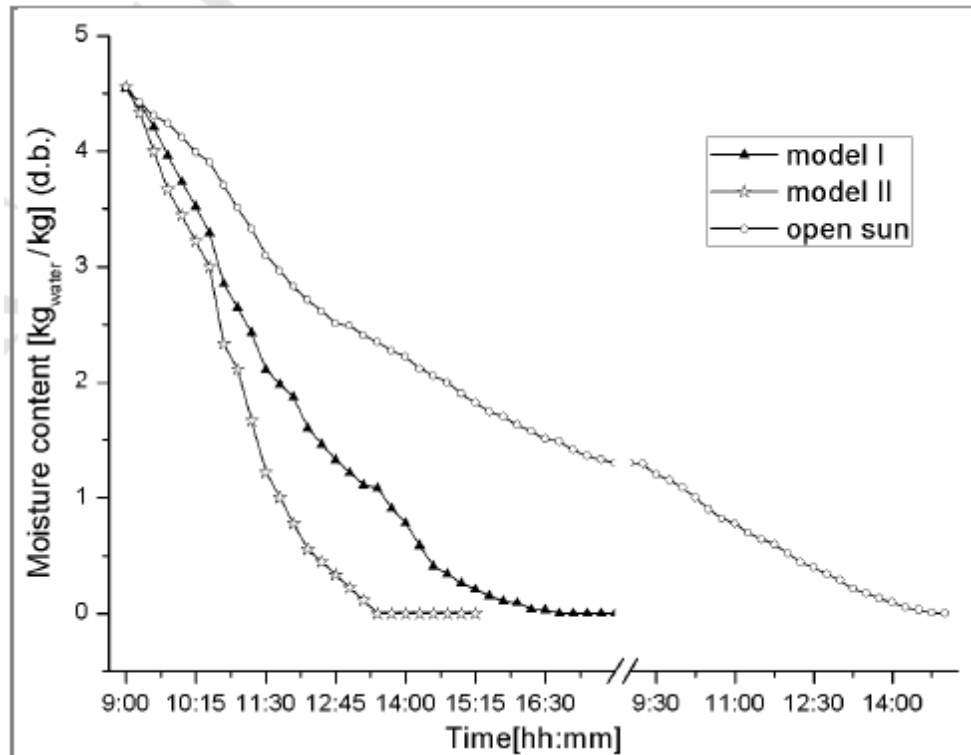
Figure I.11: Evolution of the henna moisture content (dry basis) vs. the drying time for different dryer models (m =0.024Kg/s), compared to the traditional drying [11].

    Hocine Mzad et al [12], attempted to provide a different approach in terms of efficiency improvement of solar systems. Thus, they realized and tested a solar air collector, its low cost makes it ideally suited for many applications where high efficiency is not required and low cost is important . They conclude that choosing the suitable materials of absorber, glass cover and insulation improve heat transfer in the air vein and reduce considerably top and bottom losses, and The increase of the inclination angle provides greater differences energy (deviations) due to the increase of the zenithal angle. Obviously, efficiency is dependent on the orientation of solar collectors and the measured parameters climate conditions such as wind speed, solar radiation and ambient temperature.

    Bhowmik and Amin [13], presented a new technology to improve the performance of the solar thermal collectors. They used solar reflector with the solar Flat plate collector to increase the reflectivity of the collector(shown in figure 12). Thus, the reflector concentrates both direct and diffuse radiation of the sun toward the collector. That lead to increased the quantity of radiation of sun solar on the collector. Thus, the heat transfer rate and the collector efficiency

are strongly depending on solar radiation. The collector efficiency is obtained here, without reflector as 51%, and with reflector as 61%. Thus, the overall efficiency of the flat plate solar collector is increased approximately 10% by using the reflector with the collector.
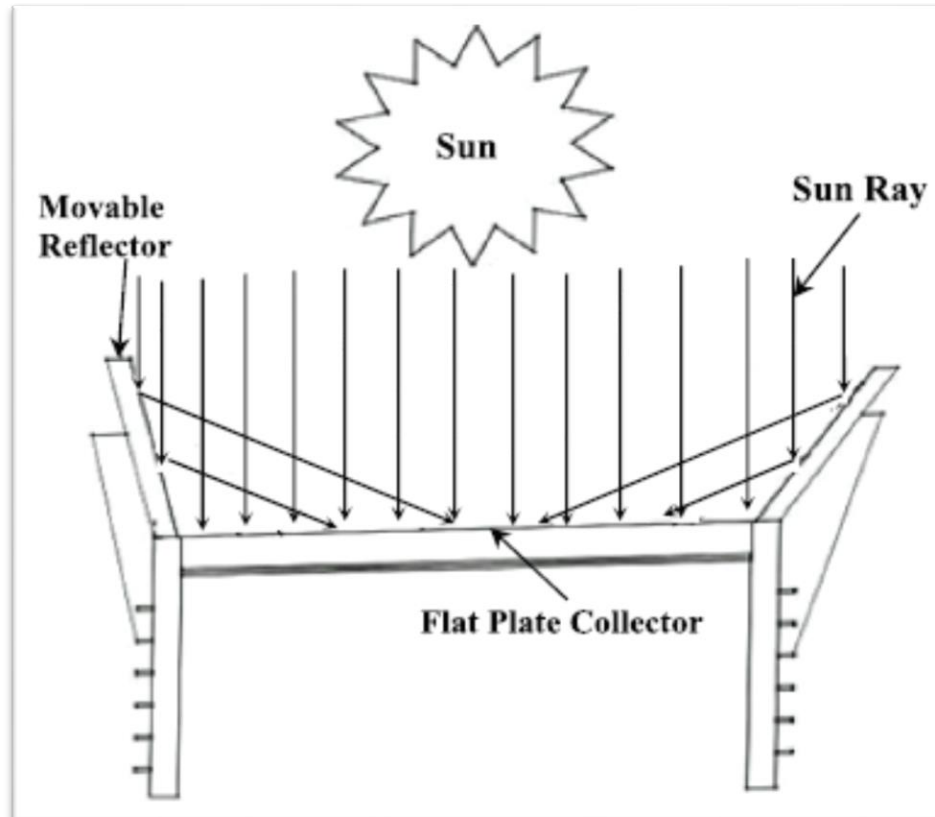
Figure I.12: The flat plate collector with reflector [13].

Wei Changa et al [14], analyzed theoretically and experimentally the thermal performance of the solar air collector with finned absorber. The results show that the error between the theory calculation model and the experiment test maintains at around 9%. They summarized that:

1. The installation angle of the fin plate air collector has little effect on the efficiency. The efficiency difference is only 3% in different angles, the error is only with 3.5% which is in permitted range (shown in figure 13).
2. The efficiency of fin plate air the collector varies significantly in different air mass flows, especially when the working medium mass flow is small and increases slowly (shown in figure 14).
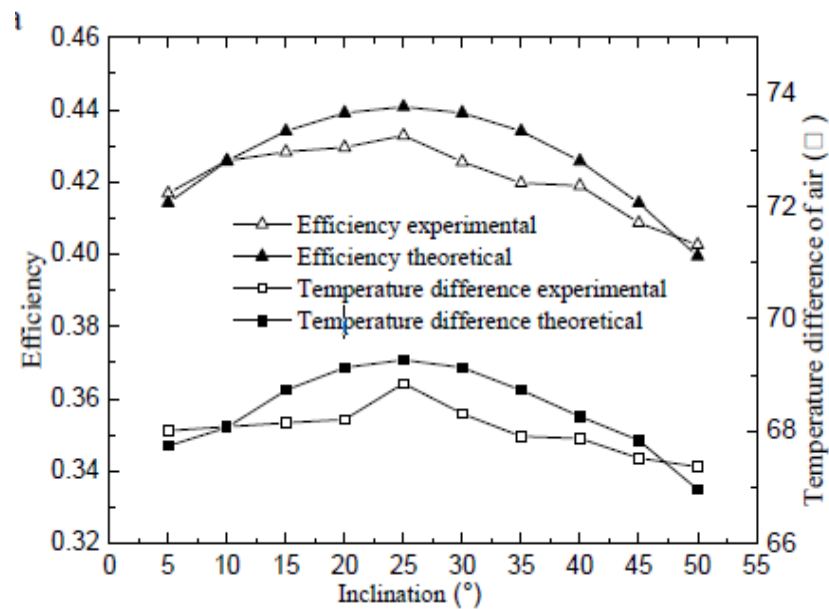
Figure I.13: The value of import and export temperature difference of collector efficiency in different inclination [14].
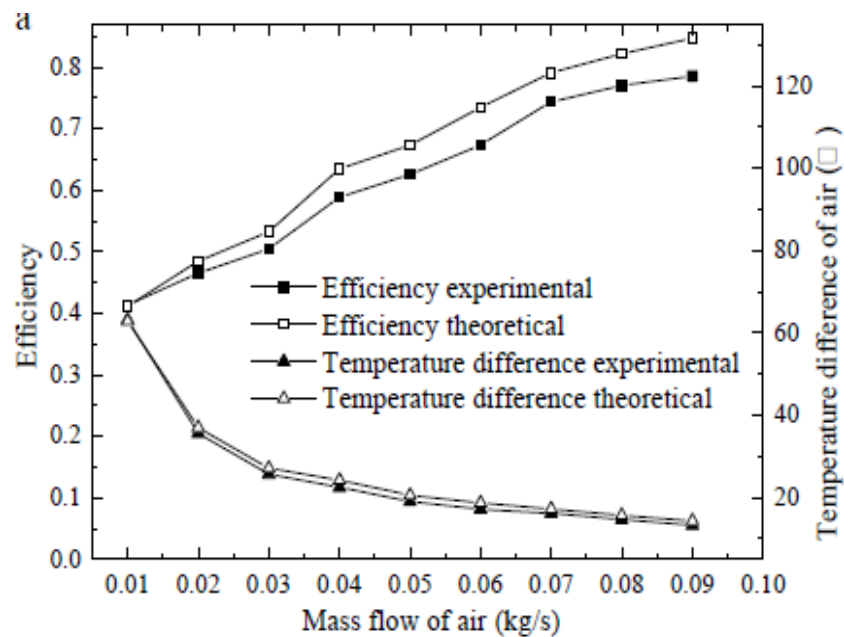
Figure I.14: The impact of air mass flow on the collector efficiency and temperature difference[14].

Cuzminschi et al [15], investigated an innovative design of solar air heater and justified it by a Computational Fluid Dynamics (CFD)simulation, implementing and experimentally testing

a sample. they tested the functionality of their sample of the solar air heater for 50 weeks and obtained an agreement between the results of the numerical simulation, implemented using Open FOAM (an open source numerical CFD software) and the experimental results. They found that the analysis of numerical simulations and experimental data lead to conclude that this product can be used as an air heating system for residential and office buildings. It is also very suitable for green-houses heating, due to it working upon the principle of natural convection, to avoid airstreams and their negative effect on plant growth. The device can be used as a heating and ventilation system depending on the needs of the user. Also, this solar air heater can replace the heating system during the autumn-spring period when the outdoor temperature is above−10◦C.

Moummi et al [16], studied the improvement of the efficiency factor for the solar collectors, they made an increasingly turbulent flow between the absorber and the back wooden plate. So, they used deterrents of different structures. In their study, they chosed rectangular plate fins inserted perpendicular to the flow and they noted that the introduction of these fins make it possible to reduce the expenditure generated to transport the air. Thus, at the end of their study, they summarized through the experiments that, the addition of fins increases the heat transfer. As for the absorber selectivity, it does not represent a remarkable improvement in the presence of fins. They explained that by the fact that the nonselective absorber warms up in the absence of fins , therefore there are more thermal losses, whereas if the absorber is selective, the losses are generally little and the difference of the coefficients of emission is repaid by the presence of fins which cool the absorber.

Labed et al [17]**,** studied the feasibility of a solar powered solid desiccant system (figure 15) in Algerian Sahara, particularly in the region of Biskra, with low generation temperatures (50-80 °C). They experimentally evaluated the performances of flat plate solar air heaters as an important component of the open-cycle dehumidification-humidification process. They noted that the air humidity in the building will be higher than the acceptable comfort conditions for the Pennington cycle in this climatic conditions (Tamb=40 °C, RH=30 %), so they suggested that if they used the Dynkel model for the same climatic conditions, the solid desiccant cooling system can show a suitable blowing conditions in the building, and they investigated the applicability of the Dynkel model in summer in very hot days (Tamb >> 40°C). In this

investigation, the authors demonstrated that; the temperature accomplished by the solar FPCs in a huge band of air flow rate can fulfill the energy needs for the dehumidification of desiccant wheel.
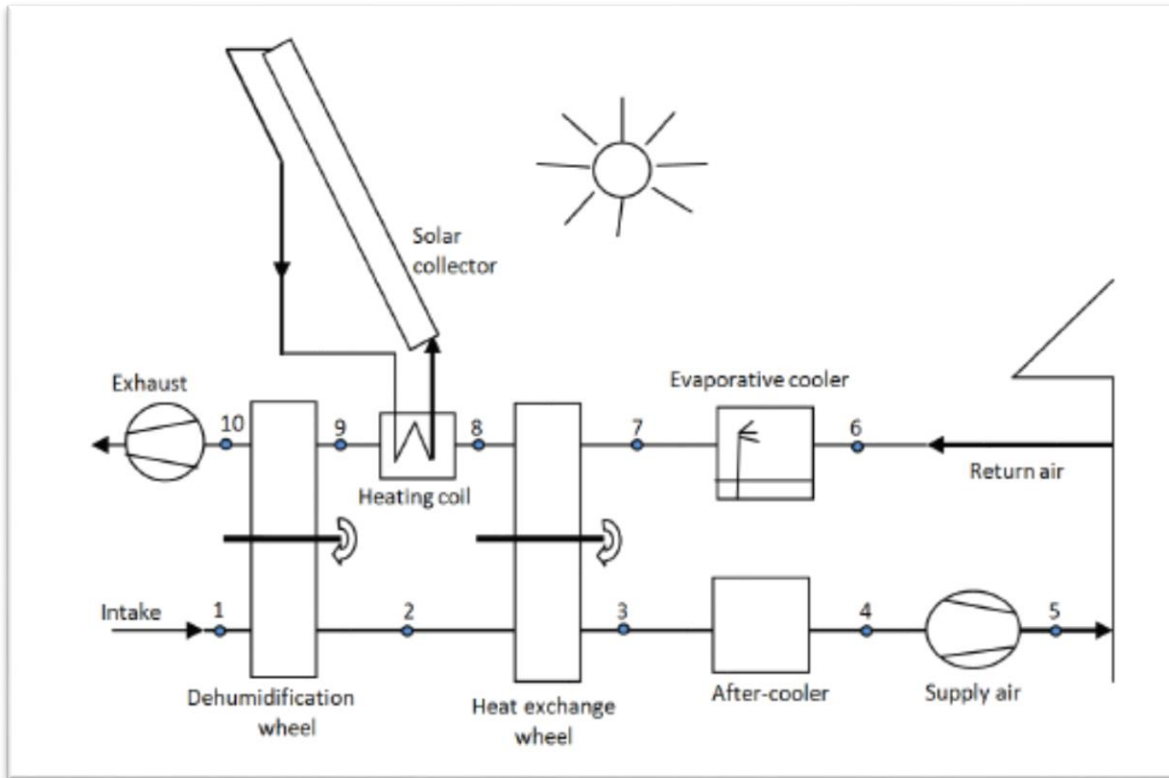
Figure I.15: A solid desiccant cooling system with solar collector(Pennington cycle) [17].

Saxena et al [18]**,** evaluated the performances of Solar air heaters different applications, such as: drying, timber seasoning and space heating. The solar air heater (SAH) has been intended to deliver a decent exhaust temperature for long hours particularly on account of poor surrounding conditions or amid off daylight hours. A mixture of desert and granular carbon in the ratio of 4:6 has been used as thermal heat storage inside the SAH. Two halogen lights of 300 W are used to increase the exhaust temperature of the SAH by placing them in the inlet and outlet ducts. All the experiments are conducted on natural and forced convection for performance evaluation on two similar design solar air heaters (with and without heat storage). The authors compared between two similar design of solar air heaters; carrying desert and granular carbon to find out an optimum design of a SAH with long term heating and they found The

thermal efficiencies of the novel SAH range from 18.04% to 20.78% of natural convection and 52.21% −80.05% with forced convection.

Jongpluempiti et al [19], studied the design and construction of the solar air heater for spray dryer of region Thailand. They showed the relationship between the inclination angle of the flat plate solar air heater with thermal efficiency (figure 16) and their effect on the collection of sunlight. The dimension of solar air heater was 1.20m x 1.60m x 0.20m (figure 17). The FPC is composed of black galvanized steel flat plate of 3.04 square meters attached below the covered glass used as solar air collector. They found that, the inclination angle of 15 degree had a maximum temperature of 83.92 degree Celsius between 12:00 and12:30. At the same time, the hot air transfer to spray dryer was 52.58 degree Celsius, which was the best temperature of all angles.
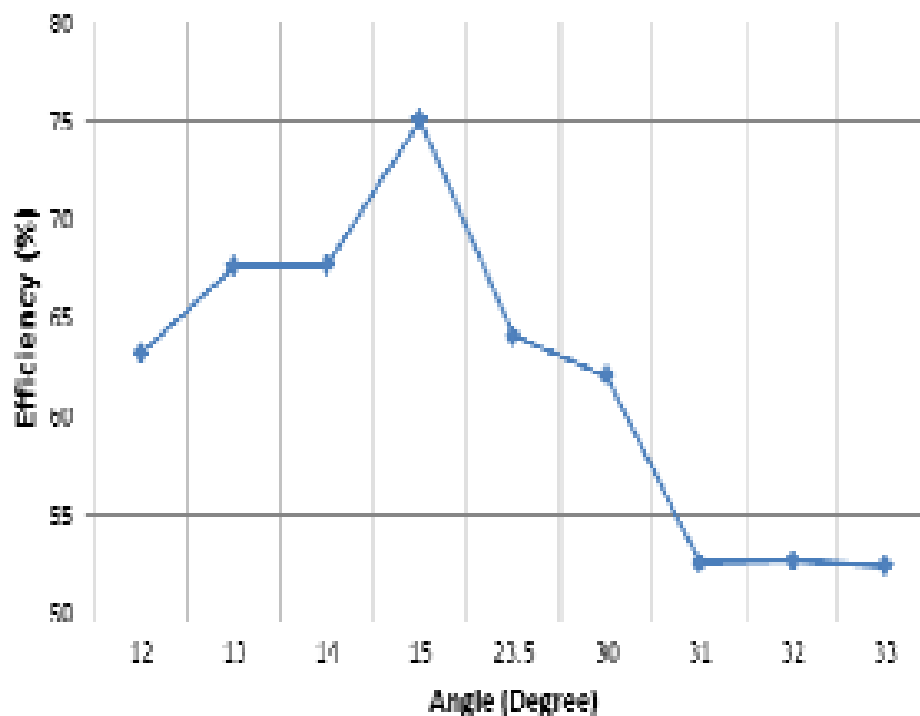
Figure I.16: Thermal efficiency and inclination angle
Relationship (region Thailand) [19].

Figure I.17: Solar air dryer [19].

I.5.Conclusion

Through this chapter which contain some previous studies about the solar air collector, we can note that, most of the investigations are focused on the improvement of the thermal efficiency of solar air collectors. We conclude that the performance of the solar air collectors depends of different parameters such as:

1. The FPC components materials properties.
2. Geometric parameters of FPC and their component.
3. Environmental conditions such as wind speed and ambient temperature.
4. The inclination angle of solar air collectors.

Chapter II: Experimental setup

II.1. Introduction

This study focused on the thermal Solar Collectors investigation. The experiments is done on a solar collector which was designed and constructed in the technological hall of the department of mechanical engineering of the University of Biskra. The tests were carried out during the period from 04 to 06 march 2019, the collector was oriented to the south face with a fixed inclination angle.

Figure II.1: The tested flat plate collector.

II.2. Experimental apparatus

II.2.1. Description of the Experimental setup

The experimental tests were carried out near to the technological hall of the department of mechanical engineering of the University of Biskra. A site located in the east south of the Algerian's Sahara at latitude 34.84522605°, a longitude of 5.74787199° and an altitude of 115m.

Figure II.2: The experiment site "Google earth".

The experimental study is realized by testing the thermal performances of the solar collector for different air mass flow rates during three days. The first day with a low mass flow rate (0.018 kg/s), the second day with a medium mass flow rate (0.024 kg/s), and the third day with a higher mass flow rate (0.033 kg/s). The experimental tests took time from 9:00 am to 16:00 pm for the three days, were the FPC is exposed directly to the sun at an inclination angle equal to the latitude.

II.2.2. Technical Characteristics of the FPC

- The main components of the FPC are:

  ➢ A transparent Plexiglas cover with a thickness of 3 mm.
  ➢ A thin galvanized steel plate (0.5mm) painted with black matte pinned in wood frame.
  ➢ The rear insulation is ensured by means of a sheet of polystyrene, 40 mm thick.
  ➢ wooden box that provides lateral isolation and keeps all thing safety.
  ➢ plywood panel (3mm) used to protect the polystyrene from external and atmospheric agents.

- Components and dimensions :

Building elements	Length (m)	Width (m)	Thickness (mm)
Transparent cover	1.7	0.9	3
Absorber	1.6	0.8	0.5
Insulation(polystyrene)	1.6	0.8	40
Wood frame	1.7	0.9	30×30

Table II.1: Dimensions of constituents.

• Thermo-physical characteristic :

Building elements	Materials	Density (kg/m3)	Specific heat (j/kg.°K)	Thermal conductivity (w/m. .°K)
Transparent cover	Plexiglas	1.2	1500	1.5
Wood frame	Wood	5100	1200	0.15
Absorber	galvanized steel	7800	473	45
Insulation	polystyrene	16	1670	0.042

Table II.2: Thermo-physical characteristics of the components.

• Optical characteristics:

Building element	Emissivity (ε)	Absorption (α)	Transmission (τ)
Transparent cover	0.9	0.5	0.9
Black painted absorber	0.95	0.9	-
Insulating	0.6	-	-

Table II.3: Optical characteristics of the building elements.

- Dimensional Characteristics:

Figure 3 represents a transversal section of the collector:
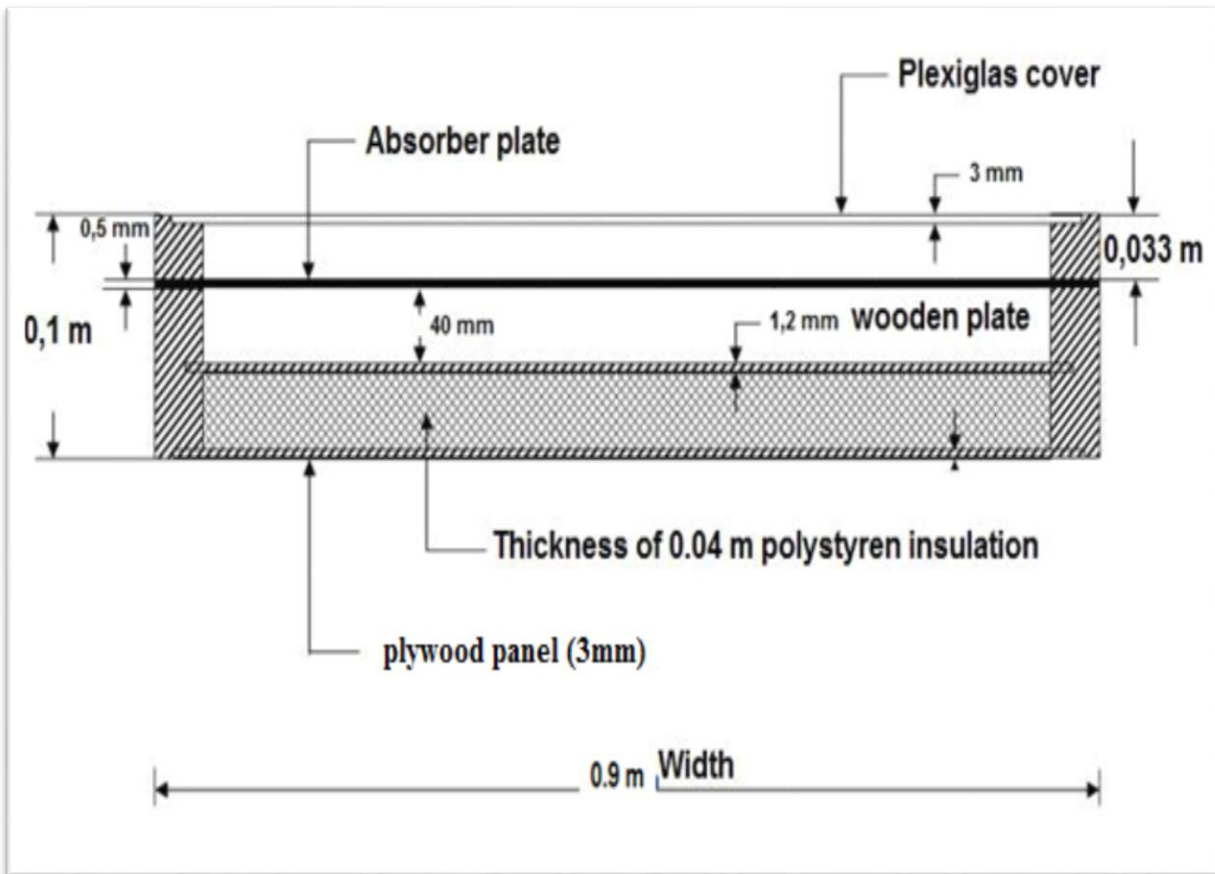
Figure II.3: Dimensional characteristics [20].

The designed solar collector consists of a 40 mm air stream located under the absorber, the distance between the absorber and the Plexiglas cover is 33 mm.

• The solar collector that we had studied presented in this diagram:
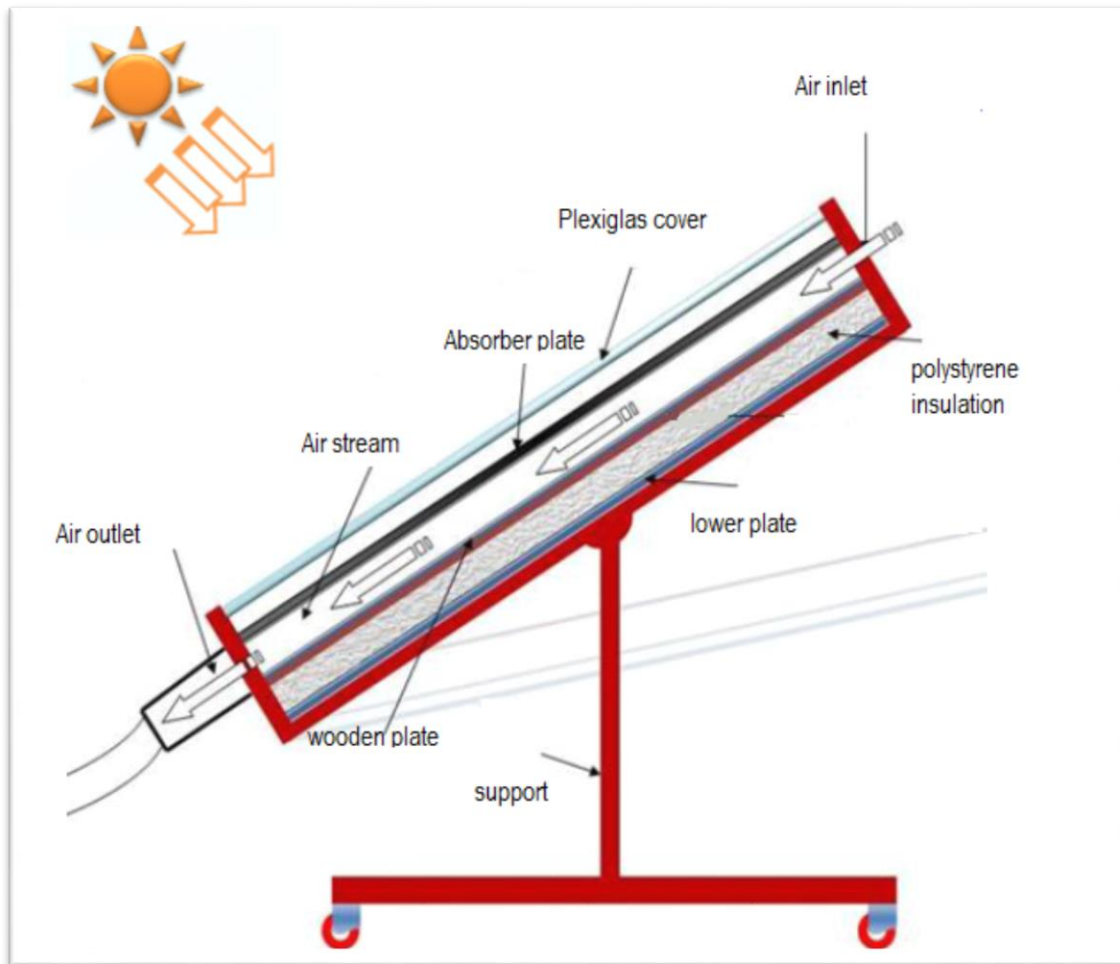
Figure II.4: A schematic view of the solar collector [20].

• The Vacuum cleaner (Fan):

For the air flow circulation we used a mobile vacuum cleaner (vacuum cleaner-1x suction Drive 1 KW Weight 30 kg) during the experiment. The machinery data:

➤ Machine type: air filter.
➤ Manufacturer: AB Lectrostatic.
➤ Model : MPF-803.
➤ Overall dimensions: depth 84cm width 32.5cm height 42.5cm.

Figure II.5: Vacuum cleaner.

II.3. Measuring instruments

➕ Flow Measurements :

For the measurement of the flow rate we used LVB THERMO-ANEMOMETER WITH PROPELLER Ø 100 MM – KIMO, some features:

➢ Power supply: 4 AAA batteries LR03 1.5 V.
➢ Air velocity: Hall Effect sensor.
➢ Ambiant temperature: CTN FPC.
➢ Operating temperature range: 0 to +50 ° C.
➢ Operating temperature range: 0 to +50 ° C.
➢ Operating temperature probe From: 0 to +50 ° C.
➢ Weight =390 g.

Figure II.6: Flow measurements device.

🞢 Measurement of solar radiation:

For measuring the global solar irradiance, the instrument (pyranometer) is equipped with a display for direct read-out of light intensity in W/m2. An analogue output signal is provided through two safety sockets on the front plate, for use with data acquisition devices, for example, some device properties:

➢ Type : Frederiksen, Hand Pyranometer, 4890.20
➢ Dimensions: 172 x 108 x 58 mm.
➢ Measurement range: 0-1999 W/m2.
➢ Resolution: 1 W/m2.
➢ Precision: +/- 5%.
➢ Output signal: 100 mV = 1000 W/m2.
➢ Battery: 1 x 9 V battery (351010).

Figure II.7: Pyranometer for measuring solar irradiance.

➕ Measurement of electrical consumption:

For measuring the electrical consumption, we have used a voltmeter (Fluke 87-V).

➕ Air circulation control:

The voltage regulator is of type 4000W AC 220V SCR for adjusting the motor speed, some properties of it :

- ➤ Operating voltage: AC 220V.
- ➤ Maximum power: 4000W.
- ➤ Voltage regulation: AC 0-220V, from 10V AC.
- ➤ Dimensions: 91 x 59 (do not include the button) x 34MM.
- ➤ Protection: Anti-peak, Surge, Absorption RC (EOC).

Figure II.8: Voltage regulator.

➕ Measurement of temperatures:

For the measurement of temperatures (ambient, outlet and of the air in the channel duct) we used a Digital Thermometer Temperature Sensor .

Figure II.9: Digital Thermometer.

II.4. Test Preparation

The following preparations were made before the tests:

- ✓ The collector is exposed in outdoor conditions.
- ✓ The inclination angle of the collector is 35 ° to the south.
- ✓ The collector has been checked for any damage or abnormality.
- ✓ The collector cover is cleaned with the utmost care.

II.5. Experimental analysis of thermal performances

The efficiency of a solar collector is defined as the ratio of the amount of useful heat collected to the total amount of solar radiation striking the collector surface during any period of time [10]:

$$\eta = \frac{Qu}{G \times A} \tag{1}$$

The mass flow rate (m) formulation is:

$$m = \rho \times v \times S \tag{2}$$

where ρ is the density of air which depends on the air temperature, v is the air speed in the channel duct of the solar collector and "S" is a measurement of the tube area .

The useful heat collected for an air-type solar collector can be expressed as:

$$Q_U = m \times C_p \times (T_{out} \_ T_{in}) \tag{3}$$

where C_P is the specific heat of the air, A is the active area of the absorber. So, the thermal efficiency of FPC becomes:

$$\eta = m .C_p \frac{(Tout \_ Tin)}{G \times A} \tag{4}$$

II.6. Experimental uncertainty analysis

To carry out these experiments, six (06) insulated digital Thermometer have been used for the local and mean temperature measurements. The six digital Thermometer were added to the air channel along the direction of flow as shown in Fig. 1. Inlet and outlet air temperatures were measured by two thermocouples and the ambient temperature was measured by a digital thermometer.
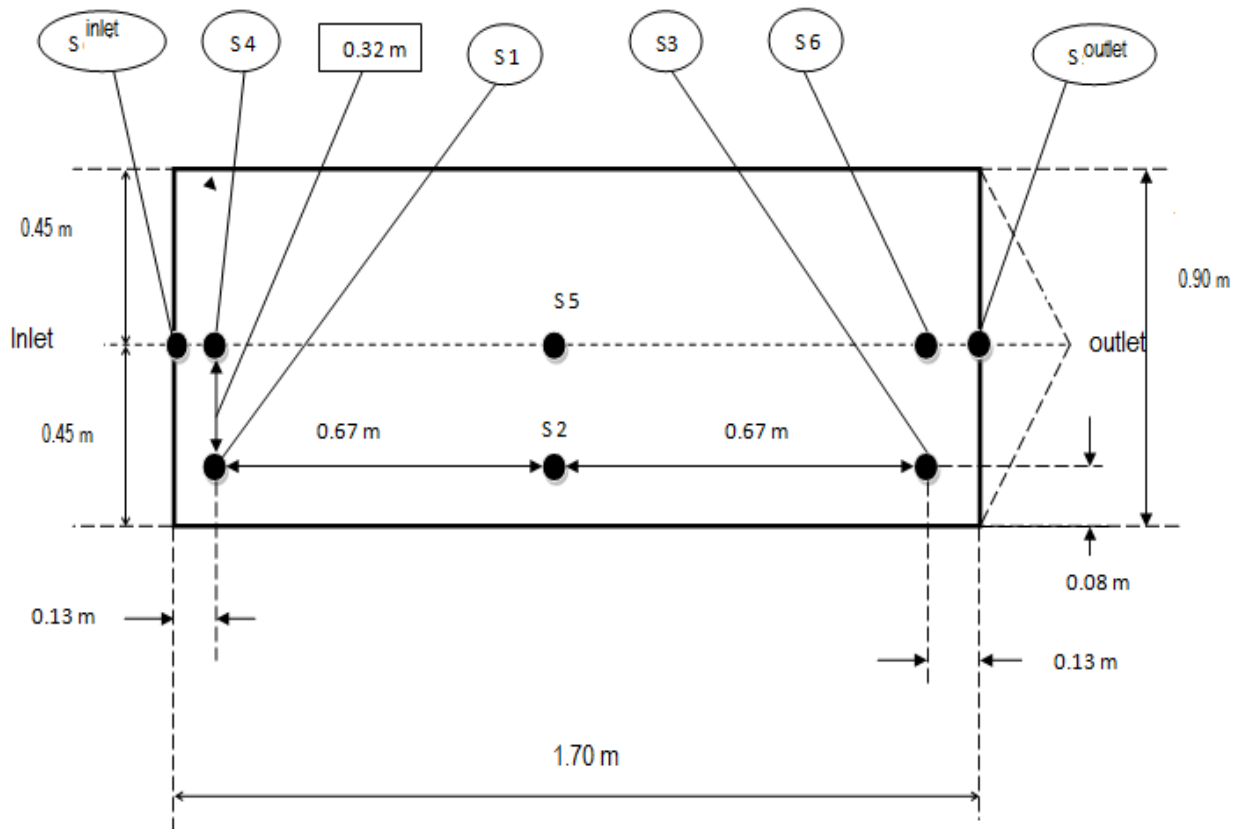
Figure II.10: Schematic view of the thermocouples positions in the FPC.

The test data were measured at an average interval of 30 min, the temperatures, solar radiation intensity, the air flow rate and wind speed are, respectively, measured with the digital thermometer with an accuracy of $0.1 \,^\circ C$, pyranometer CM 11 with 1% accuracy, a Kimo-type anemometer with hot wire (VT300) with $\pm 3\%$ of reading and $\pm 10 m^3$ for the flow rate measurement and $\pm 3\%$ of reading and $\pm\ 0.1$ m/s accuracy were used.

Based on the analysis of the errors in the experimental measurements through the use of instruments, the uncertainties in experimental measurement and results are often used to refer to possible values that may include errors. the result R of an experiment is assumed to be calculated from a set of measurements, it is given as a function of the independent variables X1, X2, . . , Xn [21].

$$R = R(X1, X2, X3, . . . , Xn) \tag{5}$$

where X1, X2, X3 are the measured variables.

Let δR be the uncertainty in the result and δX1, δX2, . . . , δXn be the uncertainties in the independent variables. If the uncertainties in the independent variables have the same odds, then uncertainty in the result having these odds is calculated by the following equation [21]:

$$\delta R = \left[\left(\frac{\partial R}{\partial X1} \ \delta X1 \right)^2 + \left(\frac{\partial R}{\partial X2} \ \delta X2 \right)^2 + \cdots + \left(\frac{\partial R}{\partial Xn} \ \delta Xn \right)^2 \right]^{\wedge 1/2} \tag{6}$$

The independent parameters measured in the experiments reported here are: collector inlet temperature Tin, collector outlet temperature Tout, ambient temperature Ta , mass flow rate and solar irradiation.

If A and C_p are considered constants in Equation (4), it can be written as:

$$\eta = f(\text{Tout, Tin, G, } m) \tag{7}$$

The total uncertainty equation for collector efficiency, can be written as:

$$\delta\eta = \left[\left(\frac{\partial \eta}{\partial m} \ \delta m \right)^2 + \left(\frac{\partial \eta}{\partial \text{Tout}} \ \delta\text{Tout} \right)^2 + \left(\frac{\partial \eta}{\partial \text{Tin}} \ \delta\text{Tin} \right)^2 + \left(\frac{\partial \eta}{\partial \text{IG}} \ \delta G \right)^2 \right]^{\wedge 1/2} \tag{8}$$

Calculations show that the total uncertainty in calculating efficiency η are almost in the order of 1%.

Chapter III:

Results and discussion

III.1. Introduction

In this chapter we present and discus the results of the tests performed on flat plat solar collector during the experimental days. The purpose of these tests is to study the thermal performances and effectiveness efficiency the studied solar FPC for different air flow rates.

This work is a part of a research project focused on the investigation of different types and configurations of FPC for many applications. The results of this study will be compared with the experimental results of a curved collector to determine the best performing collector model.

III.2. Environmental conditions

In this part we present the environmental conditions curves for different tested days:

III.2.1. The first day

The first experience is realized with a lower air flow rate (ms=0.018 kg/s), the results were taking in a clear sky. The values of solar radiation and wind speed are recorded every 30min, the experience start at 9:00 and finish at 16:00.

➢ Solar radiation:

Figure 1 represents the variation of the solar radiation as function of the time of day. By analyzing the results, we can notice that the solar radiation was about 650 w/m² at the beginning of the experience and continued increasing until reaches its limit (950 to 1000 w/m²) around 13:30, with rare passage of clouds and it begins decreasing to reach a value between 700 to 850 w/m² at 15:30.

➢ Wind speed:

Figure 2 shows the wind speed values recorded in the first testing day. It is that the wind speed is not stable. However, their values haven't exceeded three (03 m/s) in almost the experience, which make its effect without importance. Some wind speeds exceeded three (03 m/s), this can make negative effect at the instantaneous thermal performance of the flat plate

solar collectors. For that, it is preferable to realize the experimental tests in days with lower value of wind speed.
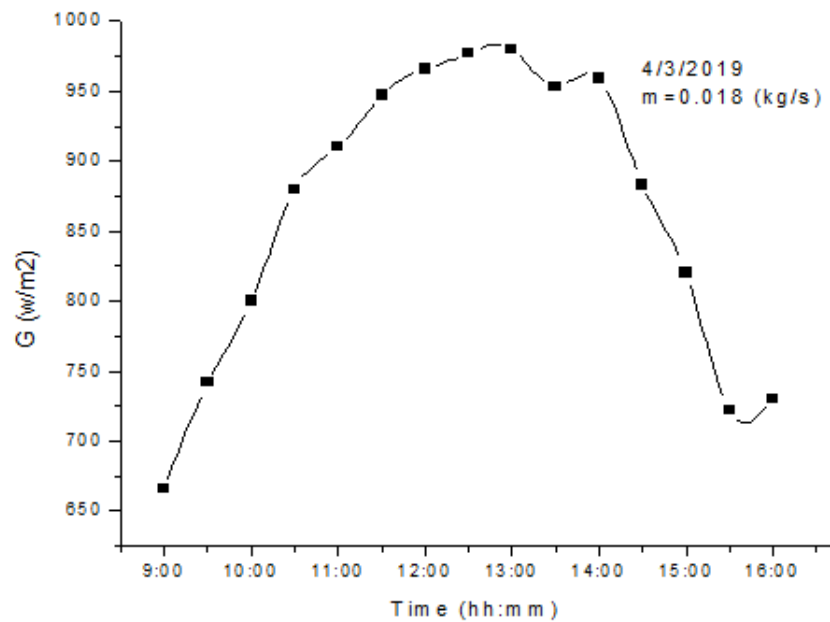
Figure III.1: Solar radiation values during the testing time(W/m2).
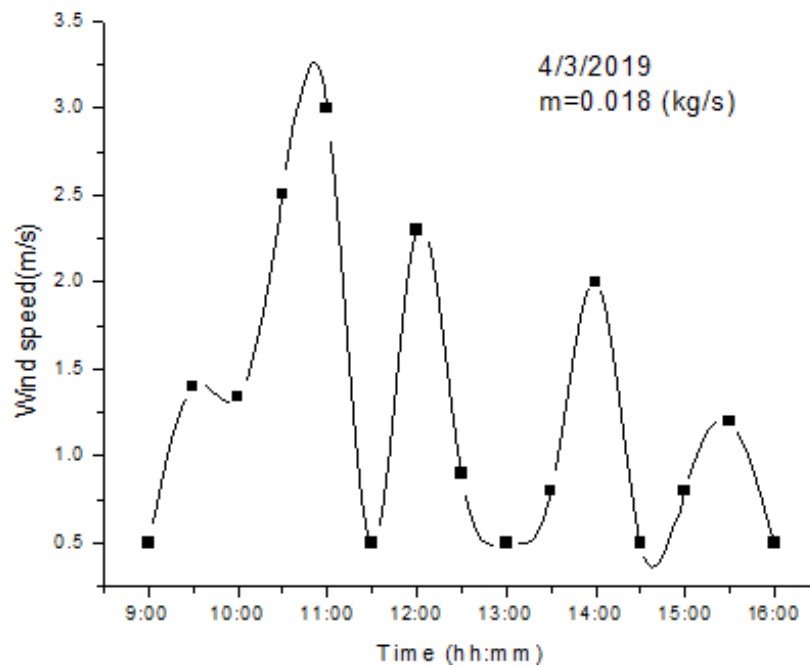
Figure III.2: Instantaneous wind speed values during testing time (m/s).

III.2.2. The second day

This experiment is realized with a medium air flow rate (ms=0.024kg/s) and almost similar to the first day conditions.

➢ Solar radiation:

Figure 3 represents the variation of the solar radiation during the time of the testing day. By analyzing the results, we found that the results in the second day are almost similar to the first day.

➢ Wind speed:

Figure 4 shows wind speed values recorded in the second testing day, we see the results are almost similar to the first day. However, their values haven't exceeded three (03 m/s) in almost the experience, which make its effect without importance.
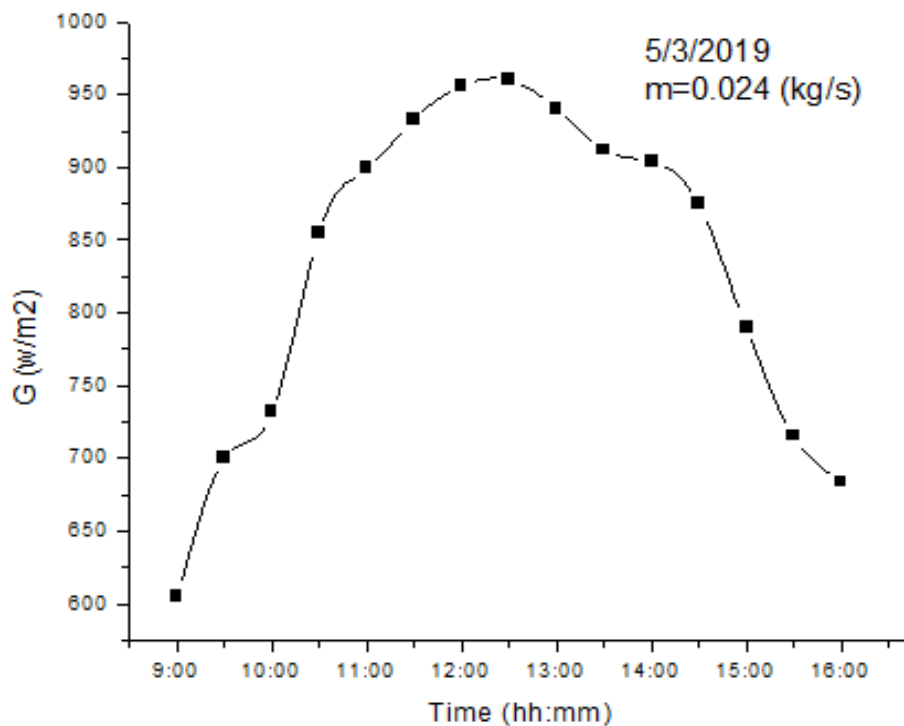
Figure III.3: Solar radiation values during the testing time (w/m2).
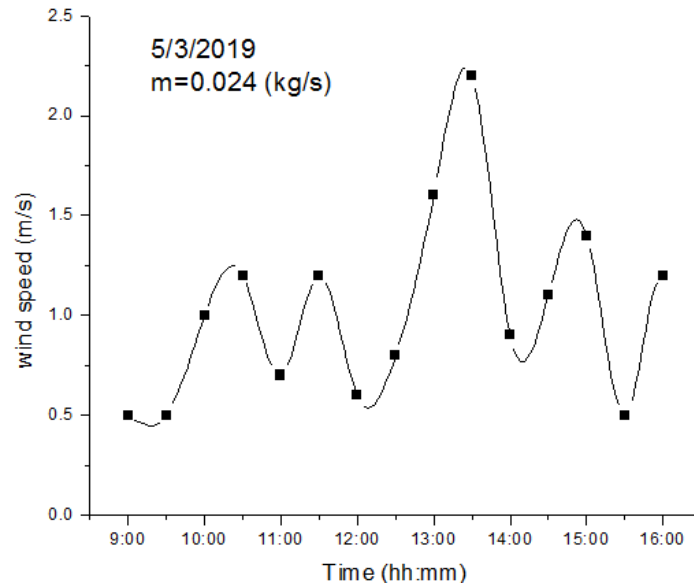
Figure III.4: Instantaneous wind speed values during testing time (m/s).

III.2.3. The third day

This experiment realized with a higher air flow rate (ms=0.033kg/s) and nearly with condition Such as the previous days of experiments.

➤ Solar radiation:

By analyzing the figure 5 we found the same notes with the previous days of experiments.
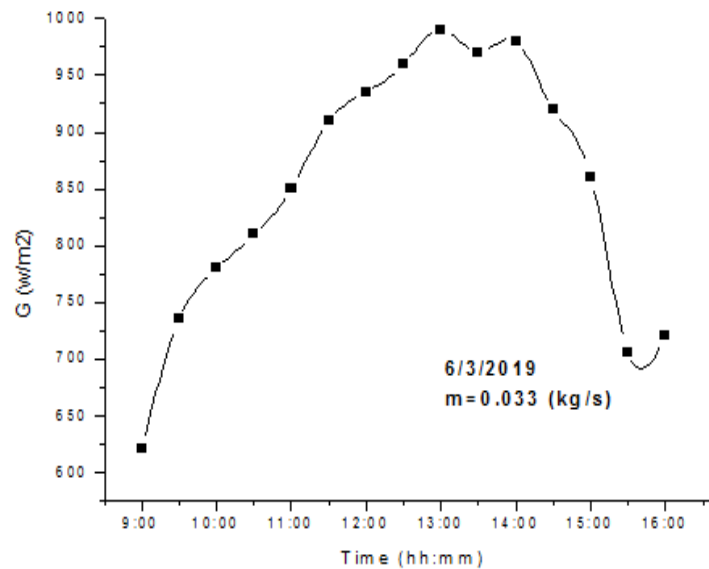
Figure III.5: Solar radiation values during the testing time(w/m²).

➢ Wind speed :

Figure 6 represents the wind speed values recorded in the third experimental day. We can see that the wind speed has an oscillating pace and it exceeds 3m/s in most of the recorded values of the day; which may be affect the thermal efficiency.
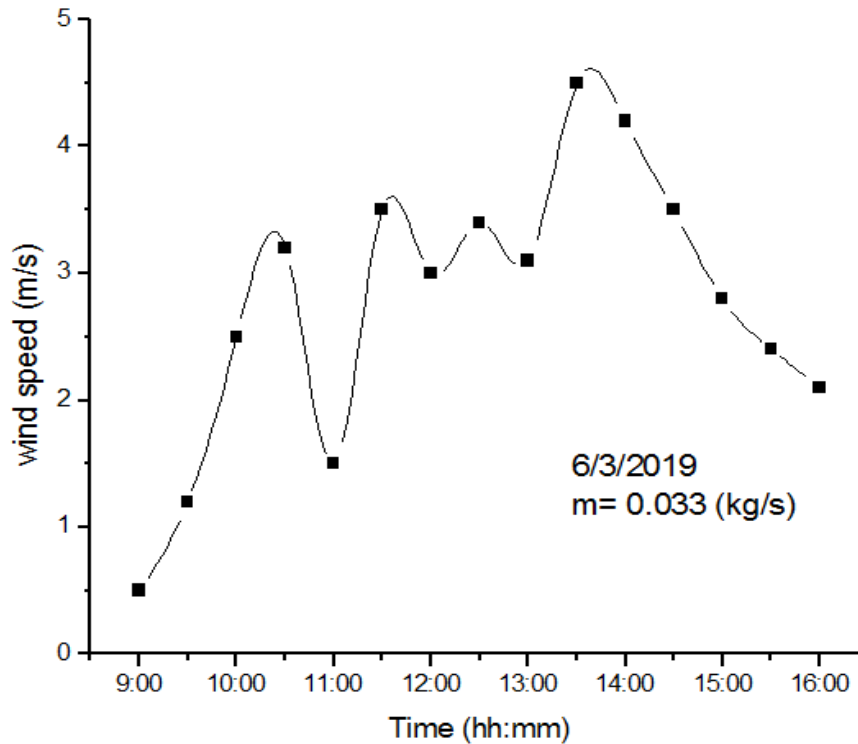
Figure III.6: Instantaneous wind speed values during testing time (m/s).

III.3. Outlet temperatures for different air flow rates

Figure 7 represents the outlet temperatures during the testing days for different air flow rates. By analyzing the results, we can notice that the outlet temperature was about 21 (°C) at   the beginning of the experience for each testing day, the outlet temperature reaches its maximum at 13:30 then it begins decreasing. We noted that the outlet temperature decrease with the increase the air flow rate.
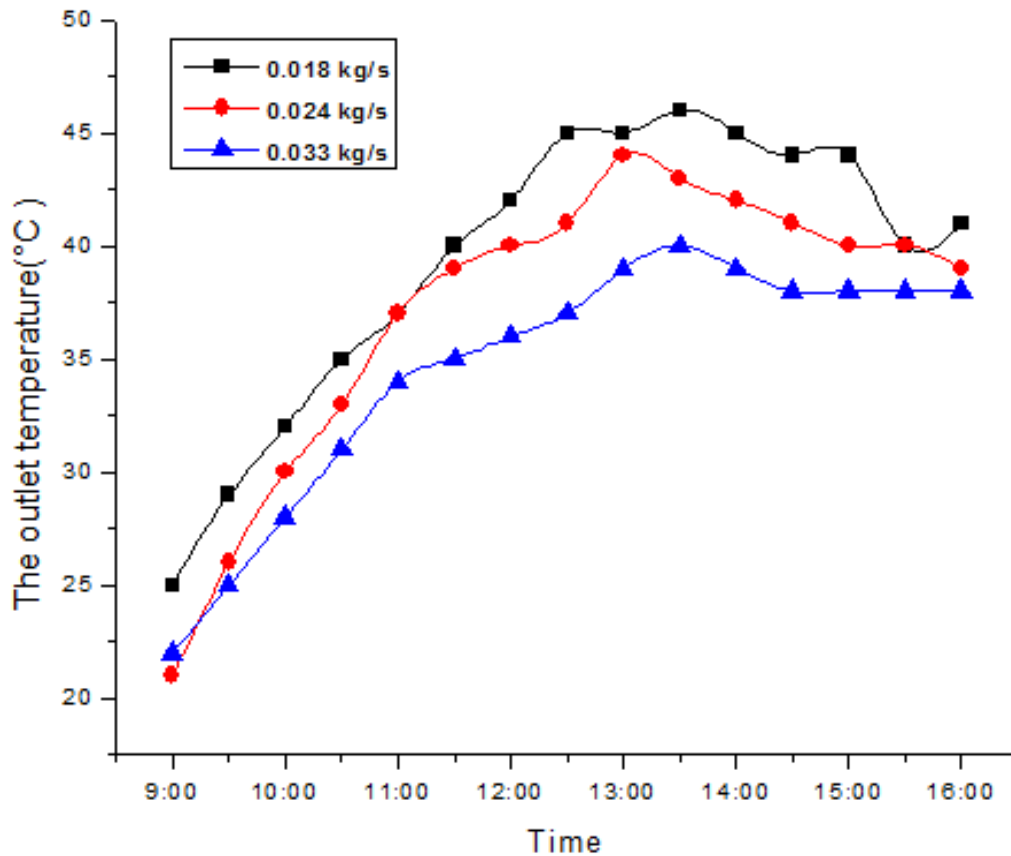
Figure III.7: The outlet temperature during testing time for different air flow rates(°C).

III.4. Thermal efficiency for different air flow rate

Figure 8 presents the thermal efficiency as function of the testing time of the experimental day. It is clear from the results that the efficiency have a lower value at the beginning of the experience, this is due to the fact that the FPC is not yet heated. The higher value of the efficiencies is recorded at 13:30 for the first day (about 38%), then starts decreasing to reach the value of 34% at the end of the experience. In the second day, with medium air flow rate, the thermal efficiency have lower value at 9:00. Then, it increased gradually to reach its maximum 40 % at 14:00. Similar remarks are noticed for the third day, with a maximum value of thermal efficiency of about (44%) which is due to the increase in the air flow rate although the high values of wind speed.
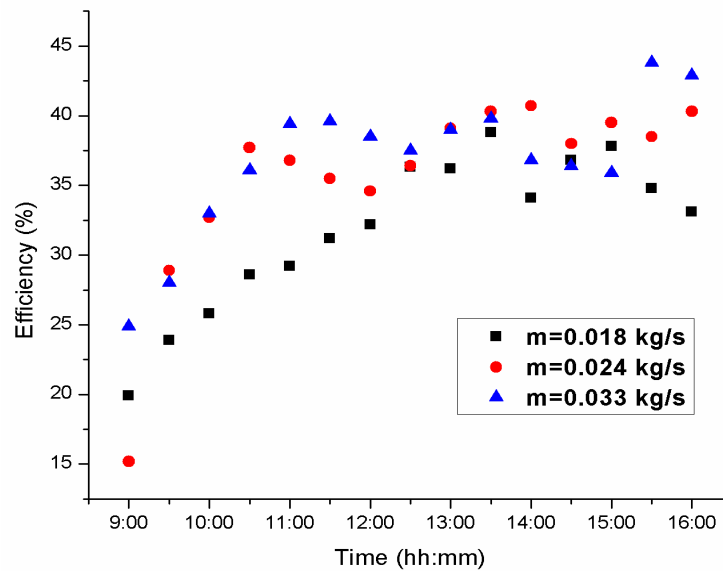
Figure III.8: The thermal efficiency for different air flow rate.

III.5. The thermal performances as function of different parameters

➢ **The thermal efficiency as function of ΔT/G**

Figures (9,10 and 11) show the variation of the thermal efficiency as a function of the characteristic parameter ΔT/G for the three air flow rates studied. This variation of the thermal efficiency as a function of ΔT/G is interesting because it makes it possible to analyze the thermal performances of the FPC under different climatic conditions.
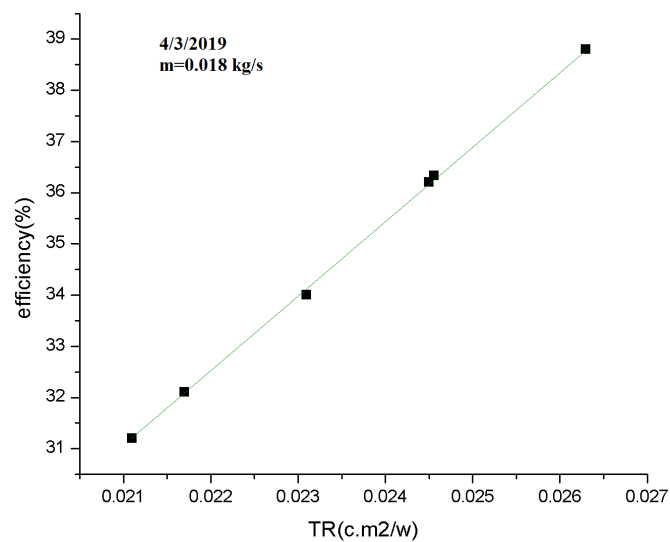
Figure III.9: The variation of the thermal efficiency as a function of ΔT/G for m=0.018 kg/s.
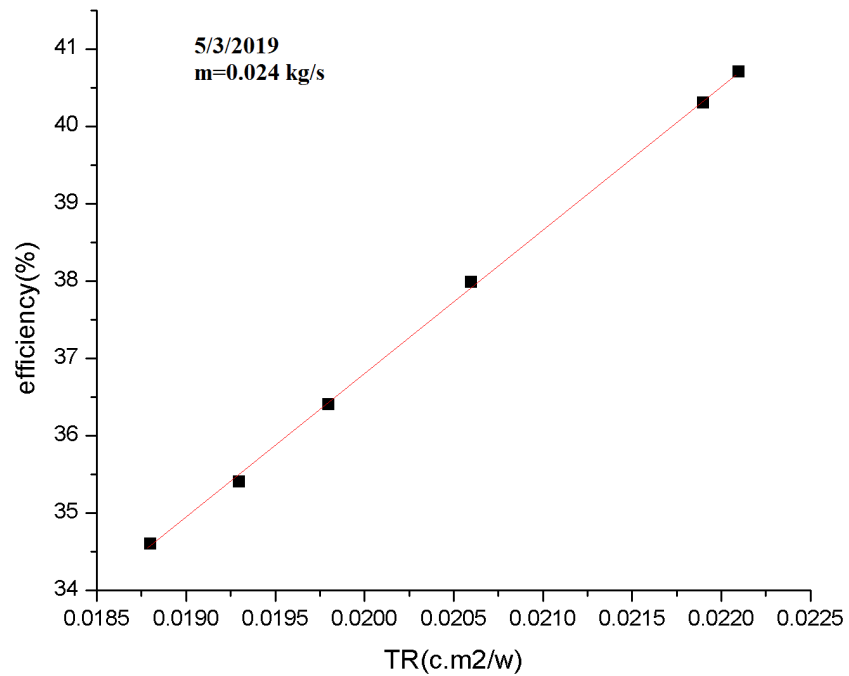
Figure III.10: The variation of the thermal efficiency as a function of $\Delta T/G$ for m=0.024 kg/s.
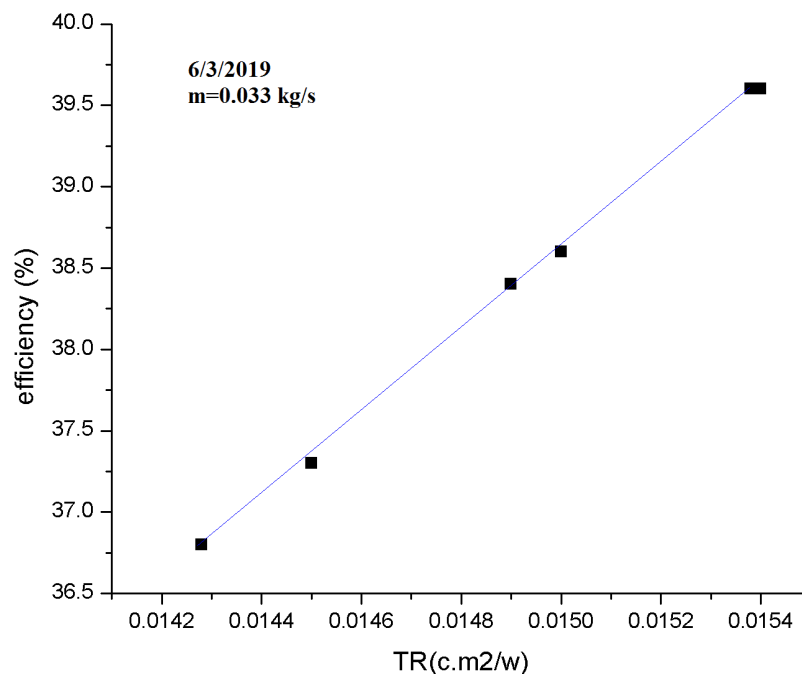
Figure III.11: The variation of the thermal efficiency as a function of $\Delta T/G$ for m=0.033 kg/s.

➢ **Temperature differences as a function of solar irradiation**

The temperature difference ($\Delta T = T_{out} - T_{in}$) is proportional to the solar radiation which gives an idea on the strong link that exists between this difference in temperature and the intensity of solar radiation. The slope is equal to 0.031 for the present study, however it was and 0.030 for the study of Labed (2012) [22]. Assuming that the ambient temperature is equal to the air temperature at the entrance of the FPC.
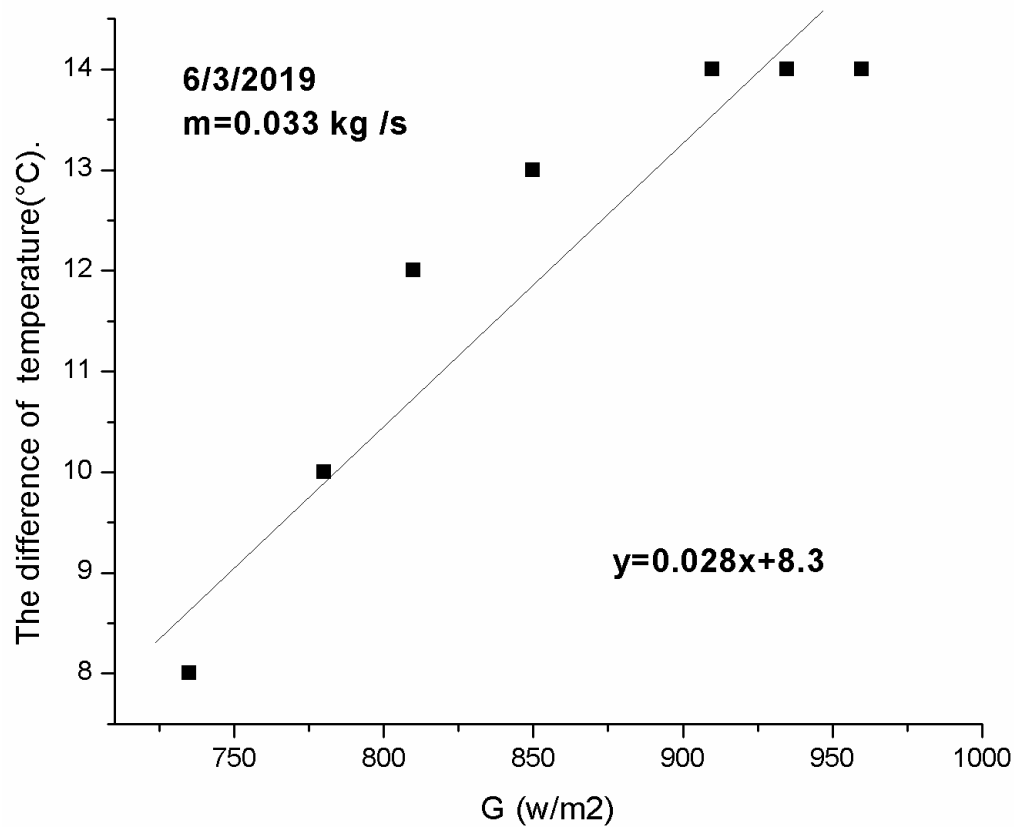
Figure III.12: Outlet temperature as function of solar radiation of the present study (m=0.033 kg/s).
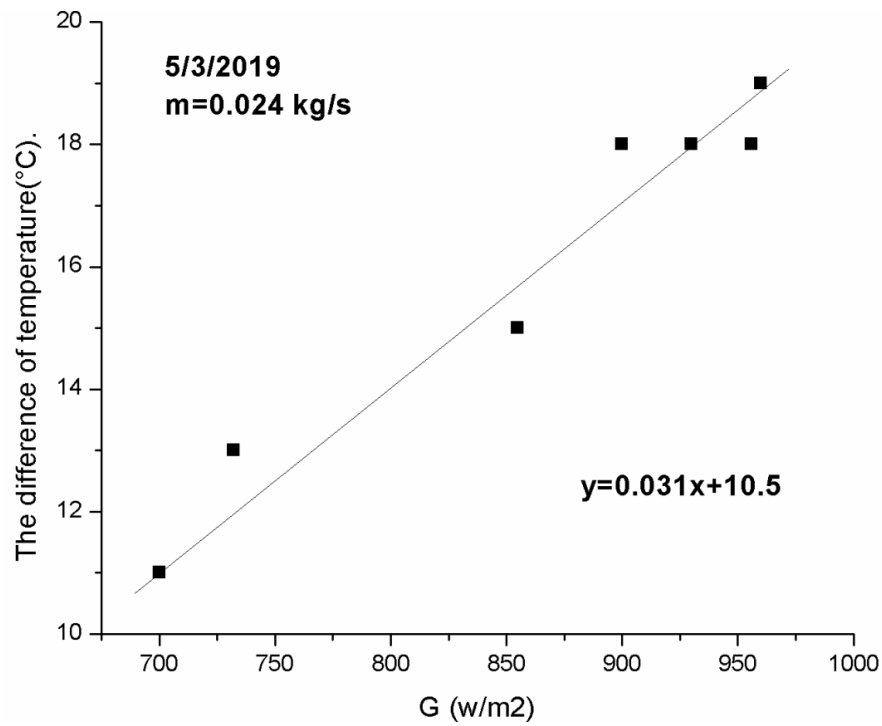
Figure III.13: Outlet temperature as function of solar radiation of the present study (m=0.024 kg/s).
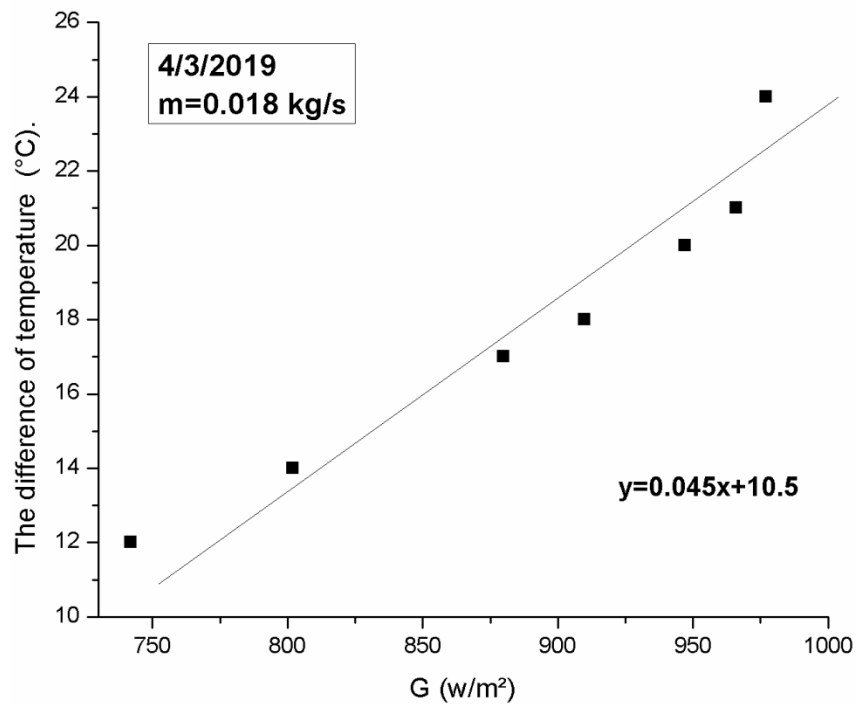
Figure III.14: Outlet temperature as function of solar radiation of the present study (m=0.018 kg/s).
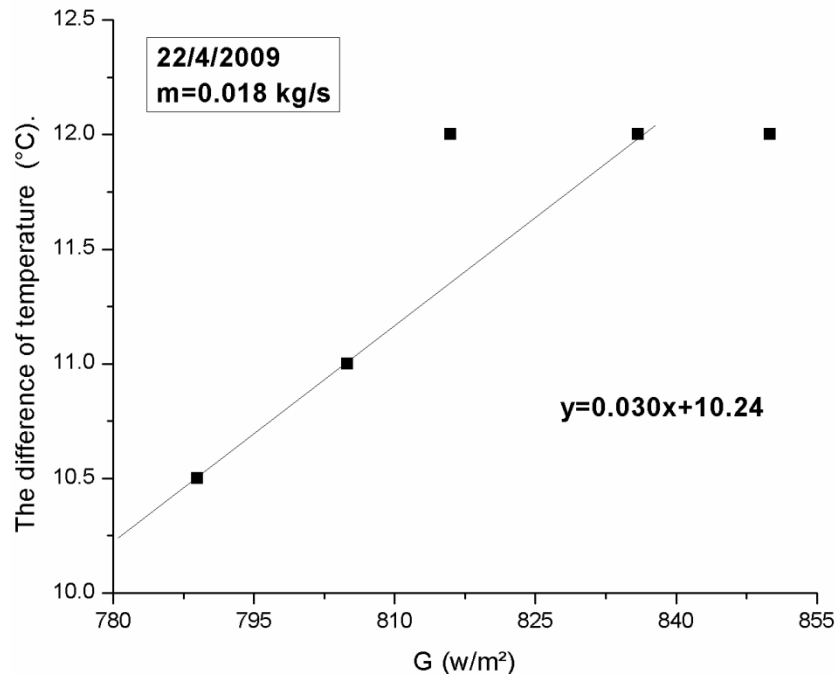
Figure III.15: Outlet temperature as function of solar radiation of Labed study [22] (m=0.018 kg/s).

III.6. Power consumption, thermal and effectiveness efficiencies for different air flow rates

To get an idea about the effect of the air flow rate on the FPC performances, we present a comparison between the results of the experiments for three air flow rates. However, this comparison include the outlet temperature level, the thermal efficiencies, the electrical power consumption, the effectiveness efficiency and temperatures distribution. We note here that, the effectiveness efficiency of the FPC is calculated from measuring the electrical consumption of the vacuum cleaner.

The variation of the thermal efficiency average (η) is expressed as a function of the variation in the air flow rate (Figure 16). It should be noticed that the thermal efficiency increased considerably with increasing air flow rate, its curve increase as a convex pace. The same evolution occurred for the electrical consumption values, we see that the power consumption increased gradually with increasing air flow rate, however, its curve increases as a concave pace, this directly affect the effectiveness efficiency which increases with increasing the flow rate as straight line curve.

Average efficiencies for different air flow rates:
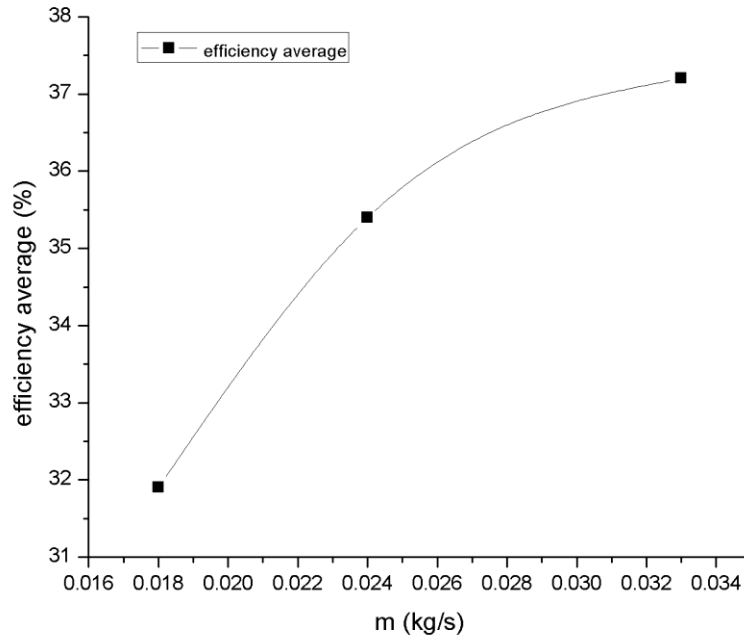
Figure III.16: Thermal efficiency average Vs air mass flow rate.

The electrical consumption for different air flow rates:
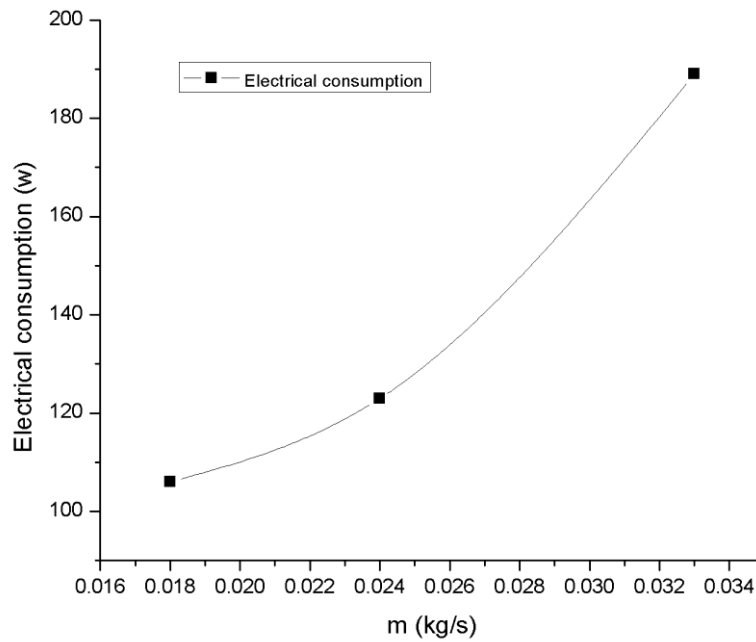
Figure III.17: Electrical consumption Vs air mass flow rate.

The effectiveness efficiencies average for different air flow rates:
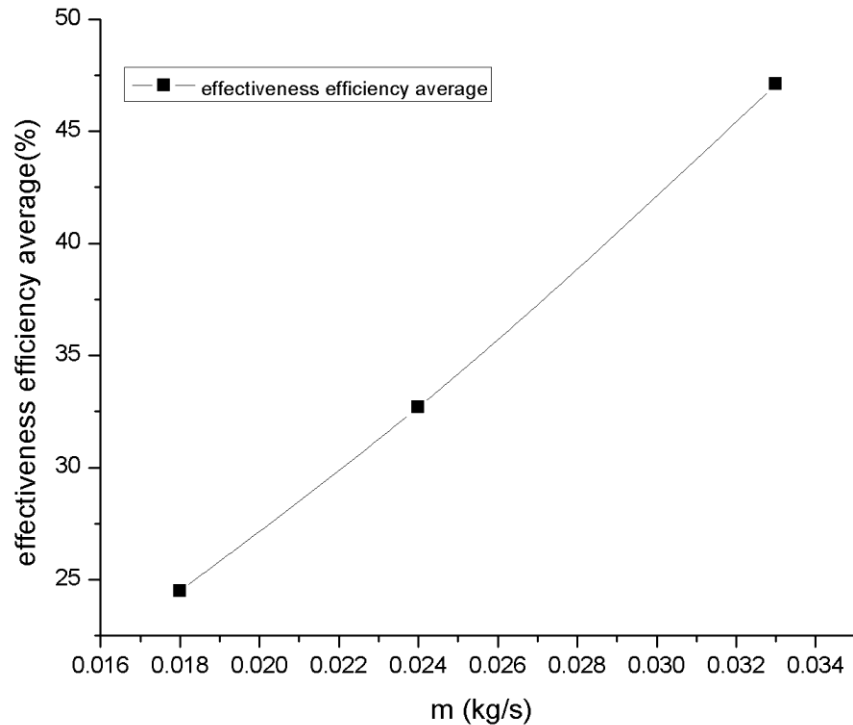
Figure III.18: Effectiveness efficiency average Vs air mass flow rate.

III.7. Temperature distribution for different air flow rates

To get an idea of the air temperature distribution in the flow channel for different air flow rates, we installed six digital thermometer in half-width of the air duct (by considering that the distribution is symmetric) as shown in chapter 2.

The temperature distribution is obtained by reading temperatures values by Digital Thermometer Sensor (TMP-10). Figures 19 (a ,b and c) show the contours of the temperature distribution of the air in the channel ducts for three different air mass flow rates; 0.018 ,0.024 and 0.033 kg/s, respectively.

It can be seen that the temperature distribution is not the same, neither at the entrance or the middle, nor at the outlet of the channel duct. We also see that, the maximum value of temperature is recorded in the outlet of FPC, the temperature of the

central line is higher than that of side parts and the temperature is more distributed for the case of the third air flow rate (0.033kg/s) in comparison with the tow other cases.
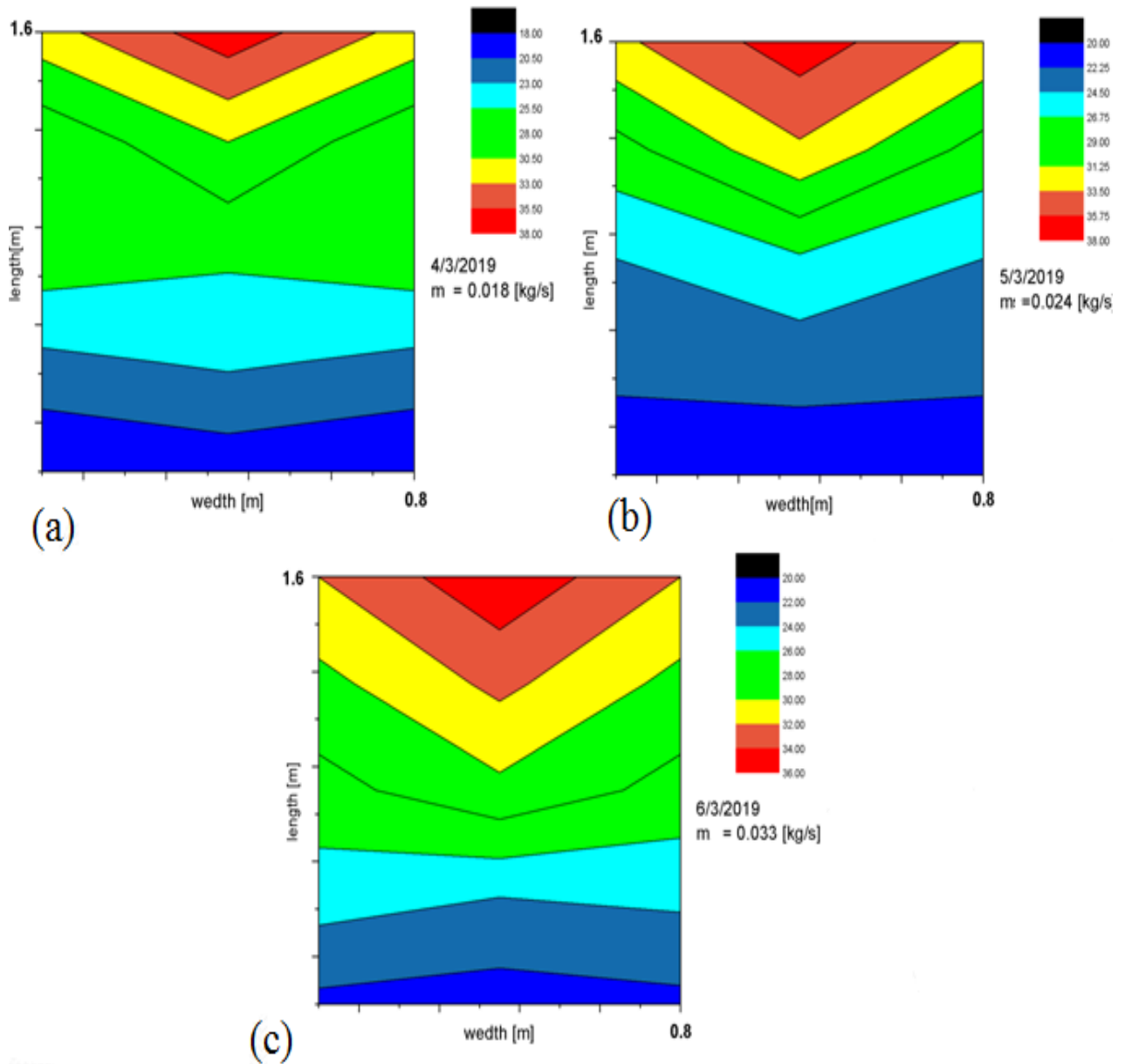
Figure III.19: Air temperature distribution in the flow channel duct for different air flow rates.

III.8. Conclusion

This experimental study is part of the experimental and numerical investigations realized by the researchers of the mechanical engineering department of Biskra University on the improvement of FPC performances.

It turns out through these results that the thermal efficiency increases gradually with increasing air flow rate.

The same evolution occurred for the electrical consumption values, we see that the power consumption increased gradually with increasing air flow rate, however, its curve increases as a concave pace, this directly affect the effectiveness efficiency which increases with increasing the flow rate as straight line curve.

The slope of the curves (ΔT Vs G) can give an idea on the strong link that exists between this difference in temperature and the intensity of solar radiation; from the figures curves, it could be noted that, the temperature difference ($\Delta T = T_{out} - T_{in}$) is proportional to the solar radiation.

It can be seen that the temperature distribution is not the same, neither at the entrance or the middle, nor at the outlet of the channel duct. We also see that, the maximum value of temperature is recorded in the outlet of FPC, the temperature of the central line is higher than that of side parts and the temperature is more distributed for the case of the third air flow rate (0.033kg/s) in comparison with the tow other cases.

We note that these temperature distribution values are measured at about 1cm under the absorber plate. Obviously, these values are not the same for other distances. The level of temperature in the channel duct is the average temperature for different distances from the absorber plate. For that this distribution cannot be considered as a temperature level.

conclusion

Conclusion

*T*he use of solar energy in air conditioning systems in Algeria knows a remarkable development due to the high cost and the environmental problems caused by the intensive use of fossil fuels in conventional systems.

In this study, we have studied experimentally the thermal performances of a solar flat plate collector in the region of Biskra, with different air flow rates.

The solar collectors is designed, constructed and tested at the University of Biskra (Algeria) under similar environmental conditions, in a stand facing South at an inclination angle equal to the local latitude. The absorber plate was placed behind the transparent cover (Plexiglas) with a layer of static air separating it from the cover. The heated air flows between the inner surface of the absorber plate and the back surface of the channel duct.

Using the experiments undertaken, we measured: the solar radiation, wind velocity, temperature of the atmosphere air, inlet and outlet air temperatures, air temperature in the channel duct and the air mass flow rate.

Through the experiments undertaken, it can be noted that, the convective heat transfer increases with the increase in the air flow rate. This is explained by the fact that the perturbations in the air flow permit acquiring the maximum of heat from the absorber plate.

It arises from the recorded values that, the thermal efficiency increased considerably with increasing air flow rate, its curve increase as a convex pace. The same evolution occurred for the electrical consumption values, we see that the power consumption increased gradually with increasing air flow rate, however, its curve increases as a concave pace, this directly affect the effectiveness efficiency which increases with increasing the flow rate as straight line curve. We note here that, the effectiveness efficiency of the FPC is calculated from measuring the electrical consumption of the vacuum cleaner.

References:

[1] Goswami DY. Principles of solar engineering. CRC Press; 2015 Feb 20.

[2] Haroun B, Etude expérimentale de deux types de capteurs solaires plan et curviligne, master thesis, University of Biskra, 2017.

[3] Mosleh A, Wild ali H, Under floor heating system, master thesis, Al-Najah University of Palestine, 2017.

[4] Foster R, Ghassemi M, Cota A. Solar energy: Renewable energy and the environment. CRC Press; 2009 Aug 18.

[5] https://energyeducation.ca/encyclopedia/Solar_collector (01/06/2019).

[6] Kalogirou SA. Solar thermal collectors and applications. Progress in energy and combustion science. 2004 Jan 1;30(3):231-95.

[7] http://www.daviddarling.info/encyclopedia/T/AE_transpired_air_collector.html (05/06/2019).

[8] Kumar R, Rosen MA. A critical review of photovoltaic–thermal solar collectors for air heating. Applied Energy. 2011 Nov 1;88(11):3603-14.

[9] Fudholi A, Sopian K. A review of solar air flat plate collector for drying application. Renewable and Sustainable Energy Reviews. 2019 Mar 1;102:333-45.

[10] Chabane F, Moummi N, Benramache S. Experimental analysis on thermal performance of a solar air collector with longitudinal fins in a region of Biskra, Algeria. Journal of Power Technologies. 2013 Mar 18;93(1):52-8.

[11] Labed A, Moummi N, Aoues K, Benchabane A. Solar drying of henna (Lawsonia inermis) using different models of solar flat plate collectors: an experimental investigation in the region of Biskra (Algeria). Journal of Cleaner Production. 2016 Jan 20;112:2545-52.

[12] Mzad H, Bey K, Khelif R. Investigative study of the thermal performance of a trial solar air heater. Case Studies in Thermal Engineering. 2019 Mar 1;13:100373.

[13] Bhowmik H, Amin R. Efficiency improvement of flat plate solar collector using reflector. Energy Reports. 2017 Nov 1;3:119-23.

[14] Chang W, Wang Y, Li M, Luo X, Ruan Y, Hong Y, Zhang S. The theoretical and experimental research on thermal performance of solar air collector with finned absorber. Energy Procedia. 2015 May 1;70:13-22.

[15] Cuzminschi M, Gherasim R, Girleanu V, Zubarev A, Stamatin I. Innovative thermo-solar air heater. Energy and Buildings. 2018 Jan 1;158:964-70.

[16] Moummi N, Youcef-Ali S, Moummi A, Desmons JY. Energy analysis of a solar air collector with rows of fins. Renewable Energy. 2004 Oct 1;29(13):2053-64.

[17] Labed A, Rouag A, Benchabane A, Moummi N, Zerouali M. Applicability of solar desiccant cooling systems in Algerian Sahara: Experimental investigation of flat plate collectors. Journal of Applied Engineering Science & Technology. 2015 Mar 10;1(2):61-9.

[18] Saxena A, Srivastava G, Tirth V. Design and thermal performance evaluation of a novel solar air heater. Renewable energy. 2015 May 1;77:501-11.

[19] Jongpluempiti J, Pannucharoenwong N, Benjapiyaporn C, Vengsungnle P. Design and construction of the flat plate solar air heater for spray dryer. Energy Procedia. 2017 Oct 1;138:288-93.

[20] Grira F, Improving thermal performance of a solar collector without and with baffles, master thesis, university of Biskra, 2017.

[21] Labed A, Moummi N, Benchabane A, Aoues K, Moummi A. Performance investigation of single-and double-pass solar air heaters through the use of various fin geometries. International Journal of Sustainable Energy. 2012 Dec 1;31(6):423-34.

[22] Labed A. Contribution à l'étude des échanges convectifs en régime transitoire dans les Capteurs Solaires Plans à air; Application au Séchage des produits agro-alimentaires, Doctorat thesis, UNIVERSITE MOHAMED KHIDER BISKRA, 2012.

ملخص:

يمثل هذا العمل دراسة تجريبية لملتقط شمسي مسطح أملس (بدون معيقات). الهدف الرئيسي من هذا العمل هو دراسة المردود الحراري و المردود الفعلي للملتقط الشمسي في تدفقات هوائية مختلفة و أيضا دراسة توزيع درجات الحرارة في مجرى الهواء للملتقط الشمسي. لقد تم إجراء هذه التجارب في ظروف مناخية طبيعية بجامعة بسكرة بالجزائر.

كلمات البحث:

الطاقة الشمسية, المجمع الشمسي المسطح, المردود الحراري, المردود الفعلي.

Abstract :

This work presents an experimental investigation of a simple flat plate solar collector without fins (FPC). The main objective of this work is to study the thermal and effectiveness efficiencies of FPC and to get an idea about the air temperature distribution in the channel duct of FPC for different air flow rates. This experiment was carried out in outdoor environmental conditions in the University of Biskra, Algeria.

Keywords:

Solar energy, flat plate collector, effectiveness efficiency, thermal performance.

Résumé:

Ce travail est une étude expérimentale des performances thermiques et du rendement effectif d'un capteur solaire plan à air sans rugosités artificielles (FPC). En plus nous avons tracé les contours présentant les valeurs des températures de l'air à l'intérieur du canal d'écoulement du FPC pour des débits différents.

Les expériences sont réalisées dans des les conditions environnementales extérieures, à l'université de Biskra, Algérie.

Mots clés :

Energie solaire, capteur solaire plan, performance thermique, rendement effective.